Pontifícia Universidade Católica
do Rio de Janeiro

Saulo Matusalém da Silva Mendes

Matrix Models Techniques and 2D Causal Quantum Gravity

Dissertação de Mestrado

Thesis presented to the Programa de Pós-Graduação em Física of the Departamento de Física do Centro Técnico Científico da PUC–Rio, as partial fulfillment of the requirements for the degree of Mestre em Física.

Advisor: Prof. Stefan Zohren

Rio de Janeiro
September 2014

Pontifícia Universidade Católica
do Rio de Janeiro

Saulo Matusalém da Silva Mendes

Matrix Models Techniques and 2D Causal Quantum Gravity

Thesis presented to the Programa de Pós-Graduação em Física of the Departamento de Física do Centro Técnico Científico da PUC-Rio, as partial fulfillment of the requirements for the degree of Mestre.

Prof. Stefan Zohren
Advisor
Departamento de Física – PUC-Rio

Prof. Hiroshi Nunokawa
Departamento de Física – PUC-Rio

Prof. Jose Abdalla Helayël-Neto
CBPF

Luis Esteban Oxman
UFF

Prof. José Eugenio Leal
Coordinator of the Centro Técnico Científico – PUC-Rio

Rio de Janeiro, September 12th, 2014.

Saulo Matusalém da Silva Mendes

The author is graduated in physics from Universidade do Estado do Rio Grande do Norte - UERN in 2011.

Bibliographic data

Mendes, Saulo Matusalém da Silva

Matrix Models Techniques and 2D Causal Quantum Gravity / Saulo Matusalém da Silva Mendes; advisor: Stefan Zohren . — 2014.
82 f. : il. ; 30 cm

1. Dissertação (Mestrado em Física) - PUC Rio, Rio de Janeiro, 2014.

Inclui bibliografia

1. Física – Teses. Modelos de Matrizes; Polinômios Ortogonais; Expansão Topológica; Limite Planar; Energia Livre; Gravidade Quântica Causal; Triangulações Dinâmicas Causais. I. Zohren, Stefan (Advisor). II. PUC Rio. Departamento de Física. III. Título.

CDD: 530

Acknowledgments

To Stefan Zohren, for he accepted to supervise me. Not only a remarkable mathematical physicist, He is a incredible human being and advisor. His knowledge of physics, patience and encouragement are inestimable, contributing incredibly to my personal growth. His advices (not restricted to physics) turned out to be as valuable as pure gold.

To José Helayël, for constant encouragement and valuable teaching.

To some of my college professors, José Ronaldo and Raimundo Silva. The first gave me much attention in my first year, further inviting me to join his work in Astrophysics. To the second, for sharing his knowledge about Non-Extensive Statistical Mechanics. To Braz Santos and Amorim for helpful discussions and advices.

To Marco Cremona, for helping me to settle in Rio de Janeiro and at PUC-Rio while he was the graduate studies coordinator of the departamento de física.

To the staff of the departamento de física of PUC-Rio for their constant help, especially Giza, Julinho, Eliane and Márcia.

To all my colleagues of favelinha for regular discussions, times of joy and learning which I will never forget.

To CAPES for financial support.

To my mentor Rivelino Montenegro, for his invitation to science throughout my childhood and for continuous stimulation since then.

To my classroom colleagues of undergraduate studies, Paulo and Pedro Edilson, for nice discussions about physics and valuable friendship.

To my parents, Maria, Arnaldo and Sílvio. They have supported me throughout the difficult and good times and always believed in my goals.

To my brother Marcos Mendes, for financial support and great understanding of my necessities.

To my friend Alexsandro Melo, for helping me to come to Rio de Janeiro.

To my grandfather, for teaching my mother that science is worth it, although he was not formally educated.

Abstract

Mendes, Saulo Matusalém da Silva; Zohren, Stefan (Advisor). **Matrix Models Techniques and 2D Causal Quantum Gravity**. Rio de Janeiro, 2014. 82p. Dissertação de Mestrado — Departamento de Física, PUC Rio.

In this thesis we discuss the matrix models techniques applied to two dimensional quantum gravity, the dynamical triangulations (DT) approach and its causal version, so-called causal dynamical triangulations (CDT). By virtue of the Gauss-Bonnet theorem, the Einstein-Hilbert action in two dimensions becomes a topological invariant, thereupon the evaluation of the path integral becomes a simple combinatorial counting problem of graphs drawn on a Riemann surface, which leads to a topological expansion of the partition function. Using integral methods from quantum field theory we can understand the correspondence between large N matrix models and a lattice (DT and CDT) formulation of quantum gravity, where the $N \times N$ Hermitian matrices generates planar graphs (fatgraphs). Once the matrix integral is reduced to an integral of its eigenvalues, we solve the matrix model using two techniques: Orthogonal polynomials and saddle point analysis. Using orthogonal polynomials we compute the free energy in the Large N limit for different potentials. Finally, we study DT and CDT using matrix models and further make contact with a Coulomb gas analogy.

Keywords

Matrix Models; Orthogonal Polynomials; Topological Expansion; Large N limit; Free Energy; Causal Quantum Gravity; Causal Dynamical Triangulations.

Resumo

Mendes, Saulo Matusalém da Silva; Zohren, Stefan. **Técnicas de Modelos de Matrizes e Gravidade Quântica Causal em duas Dimensões**. Rio de Janeiro, 2014. 82p. Dissertação de Mestrado — Departamento de Física, PUC Rio.

Nesta dissertação nós discutimos as técnicas de modelos de matrizes para gravidade quântica em duas dimensões, as triangulações dinâmicas (DT) e sua versão causal, chamada de triangulações dinâmicas causais (CDT). Em virtude do teorema de Gauss-Bonnet a ação de Einstein-Hilbert se torna um invariante topológico em duas dimensões, por conseguinte, a avaliação da integral de caminho se transforma em um simples problema combinatório de contagem dos diagramas desenhados em uma superfície de Riemann, o que implica numa expansão topológica da função de partição. Usando métodos de integrais da teoria quântica de campos, podemos entender a correspondência entre modelos de matrizes e a formulação em grade da gravidade quântica, onde as $N \times N$ matrizes Hermitianas geram gráficos planares. Uma vez que a integral matricial se reduz a uma integração dos seus autovalores, solucionamos o modelo matricial utilizando duas técnicas: polinômios ortogonais e a análise do ponto de sela. Usando os polinômios ortogonais calculamos a energia livre no limite planar para diferentes potenciais. Por fim, partindo dos modelos matriciais estudamos DT e CDT numa analogia com o gás de Coulomb.

Palavras–chave

Modelos de Matrizes; Polinômios Ortogonais; Expansão Topológica; Limite Planar; Energia Livre; Gravidade Quântica Causal; Triangulações Dinâmicas Causais.

Contents

List of Figures

Surely there is a mine for silver, and a place for gold that they refine. Iron is taken out of the earth, and cooper is smelted from the ore...But where shall wisdom be found? And where is the place of understanding? Man does not know its worth, and it is not found in the land of the living...It cannot be bought for gold, and silver cannot be weighed its price...From where, then, does wisdom come? And where is the place of understanding?...God understands the way to it, and he knows its place. For he looks to the ends of the earth and sees everything under the heavens...Behold, the fear of the Lord, that is wisdom, and to shun evil is understanding.

Job 28, *Bible.*

1
Introduction

One of the prominent challenges of contemporary theoretical physics is the pursuit of a quantum theory of gravity, yet there are plenty of inconsistencies between the two theories [1, 2, 3]. Since the emergence of QFT, many physicists tried to apply conceptual and technical foundations of quantum mechanics to gravity. However, gravity has shown to be harder to be understood in the quantum level than the other three forces, which have all been described successfully through a quantum field theory by the end of forties (QED) and in the seventies (QCD). Due the fact that both electromagnetism and general relativity are classical field theories, and the first has been fully quantized, one might expect to achieve a quantum theory of gravity following the standard methods of QFT. However, it was early realized that due the dimensional character of the gravitational coupling constant, there is a problem with renormalization. By the end of the thirties it was understood that when applying the Pauli's quantization methods to the full non-linear version of general relativity one needs background independence [4].

In the fifties two main approaches for quantum gravity became evident, the canonical approach and the covariant approach. The first was largely developed by Dirac's Hamiltonian constraint quantization [5]. In the sixties the ADM Formalism arose to simplify the approach followed by the Hamilton-Jacobi equation [6, 7], further leading to the development of the Wheeler-Dewitt equation (a.k.a WDW equation) [8]. However, the WDW equation proved to be inefficient when tackling the quantum gravity problem, until the introduction of Ashtekhar's connection variables [9], which gave their first fruits: loop-like solutions were found in the modified WDW equation [10]. These events lead to the creation of an approach called loop quantum gravity (LQG) [11]. Furthermore, the LQG quantization method was applied to cosmology [12], known as loop quantum cosmology. One of the interesting features of this theory is that the quantum geometry effects create a repulsive force when the energy density of the spacetime reaches its maximum (This upper bound comes from LQG [13, 14]), which can be neglected at low energy scales, but at Planck scales it becomes stronger than the classical gravitational force,

therefore resolving the singularities (including those of black holes) that arise in general relativity.

Another main approach of quantum gravity is the covariant method. This approach started with perturbations around a given metric quantized through the Rosenfeld-Pauli method, which was later improved by Feynman and others [1]. In the seventies Veltman and 't Hooft showed evidence for the non-renormalizability of general relativity [15]. With such an obstacle within the approach, attempts to save it showed up, among them supergravity was the most promising. Although not conceived as a quantum theory of gravity, string theory has been reformulated and joined the group of approaches to tackle the problem in the eighties [16]. Since string theory is composed by extended objects rather than point-like objects, the size of the string serves as a regulator and tames problems with renormalization. Afterwards, many types of strings were discovered as well new extended objects called branes [17]. Not long after, supergravity was added to a bigger picture called M-theory along with all types of strings, even though to this day there is no clear and complete formulation of M-theory. Nevertheless two important achievements can be mentioned. The first is the study of black hole entropy in some backgrounds that obtained the exact formula found by Hawking [18]. The second is the anti-de Sitter/conformal field theory (AdS/CFT) correspondence, which is useful to study strongly coupled gauge theories [19].

Nonetheless, there are plenty of another approaches to quantum gravity, such as twistor theory [20], which in the last decade has been aplied to string theories [21, 22, 23, 24], causal sets [25], asymptotic safety [26], group field theory [27], noncommutative geometry [28], Regge Calculus [29] and others. A more recent approach is Hořava-Lifshitz gravity [30]. First of all, it is renormalizable in four dimensions. In this theory there is an anisotropy between space and time, such that at short scales it is not Lorentz invariant, whereas it recovers Lorentz invariance at large scales. Similar to another attempts to quantize gravity with higher curvature terms, Hořava-Lifshitz applies higher order derivatives terms to spatial components only, achieving both renormalizability and unitarity. HL gravity uses the ADM formalism (decomposition of the metric) mentioned above and it does not obey usual diffeomorphism invariance, but rather a foliation preserving diffeomorphisms (which is a starting point of the theory). Another important aspect of the theory is the formulation of the spectral dimension of the universe. See [31, 32, 33] for reviews of HL gravity.

In many of the covariant approaches one aims to define a quantum theory of gravity using a Feynman's functional integral formulation: spin foams [34],

many lattice-like formulations as well as Euclidean quantum gravity [35] belong to this line of research. Dynamical triangulations (DT) is such an approach, which aims to give a non-perturbative definition of the gravitational path integral while preserving background independence. In the quantum gravity context DT began as a regularization for the bosonic string [36, 37]. The integral over the geometry of a two-dimensional surface can be discretized and defined as a sum over triangulated surfaces, then quantum gravity is recovered in the continuum limit. Even though in two dimensions we do not have any propagating degrees of freedom, it is important as a toy model, in which the continuum approach in the context of non-critical string theory is also a toy model (Liouville gravity). It was later realized that the numerical results for higher dimensional DT have a pathological behaviour [38, 39]. Thereupon, a causal version of DT was established. It is known that numerical results in CDT are well-behaved [41, 42]. For a detailed analysis of the differences between DT and CDT see [38, 43, 44, 45, 46]. In recent years physicists have found evidence of a possible connection between CDT and Hořava-Lifshitz gravity, first in [47] and later by [48, 49], where the value of the spectral dimension is the same for both theories in four dimensions as well as other similarities (such as the phase diagram), opening a new outstanding overlap of approaches to quantum gravity (similarly to the overlap between twistor theory and string theory). In this Thesis we focus on the two-dimensional problem. The connection between matrix models and the random triangulated 2D surface is the following: A matrix integral generates fatgraphs (planar graphs) that are dual graphs of the triangulation, and thus the matrix model is a powerful technique to count the number of diagrams. Accordingly, the partition function of 2D gravity can be expressed as the free energy of a hermitian matrix model. The important fact about this connection is that it agrees with the results obtained in Liouville gravity [50, 51, 52]. There is also the possibility to take into account topology change in the theory (see [53] for a detailed analysis of topology change). As a result, the aim of this work is to use matrix models techniques as a unified framework to help us to better understand the relation between DT and CDT.

This Master's thesis is organized as follows: In chapter two we present an overview of random matrices and their connection with two-dimensional quantum gravity, where we introduce the topological expansion, Euclidean quantum gravity and Liouville gravity. In chapter three we explore the basic knowledge of discrete two-dimensional quantum gravity, defined through Euclidean dynamical triangulations (DT) and Lorenztian (or causal) dynamical triangulations (CDT). In addition, the continuum limit of DT and CDT is taken to recover the Hartle-Hawking wavefunctions of quantum gravity. In

chapter four are presented the necessary techniques and machinery of matrix models that we need to apply to DT/CDT, where we assess its eigenvalue distributions and its critical points, as well as the case of pure CDT where repulsion between the eigenvalues goes to zero, interpreted as a Fermi gas at zero temperature. In chapter five we discuss the results and open problems concerning matrix models of CDT. Besides, we compute the resolvent and the eigenvalue distribution of different matrix models (especially those attributed to DT and CDT). In Appendix A we show how to reformulate the matrix integral in terms of its eigenvalues. Appendix B provides background on crucial relations of the chapter 2. Appendix C presents two important derivations of orthogonal polynomials tools and detailed calculation of free energies for different potentials along with the functions r and s for DT and CDT. In Appendix D we show how to obtain the critical point of the coupling g in a different fashion.

2
Random matrices and quantum gravity: An overview

In this chapter we present an overview of random matrix theory and its applications as well as the motivation and advantages for its usage in physics and related fields. Then we make contact with Wick's theorem which enables us to understand matrix integrals as generators of fatgraphs (oriented double lines) which are dual graphs to a the discretized surface. Following that we present Euclidean quantum gravity and a brief review of the mains aspects of Liouville theory that is necessary to further compare with the discrete version of 2D quantum gravity.

2.1
Ensembles of random matrices

Random matrix theory aims to define a probability measure over $N \times N$ matrices. Consider the matrices M are Hermitian. One can define the Gibbs measure,

$$P(M) = \frac{1}{Z} e^{-N \operatorname{tr} V(M)} dM \quad , \quad V(M) = \sum_k g_k M^k \,, \tag{2.1}$$

Where dM is the Haar measure, which is expressed as

$$dM = \prod_i^N dM_{ii} \prod_{i<j}^N d(\operatorname{Re} M_{ij}) d(\operatorname{Im} M_{ij}) \quad . \tag{2.2}$$

We will see in the next pages the different types of probability distributions and its implications. Let us discuss a simple example. We choose the function $V(M)$ to be a Gaussian potential. Notice that there are N diagonal terms and $N(N-1)/2$ terms on both lower and upper triangular parts of the matrix. In addition, note that the matrix elements are independent of each other. Alternatively, one could define a matrix G (a.k.a Ginibre matrix [54]) which is formed by a composition of the type,

$$M = M^\dagger = \frac{1}{\sqrt{2}}(G + G^\dagger) \quad , \quad G \equiv \frac{1}{\sqrt{2}}(A + iB) \,, \tag{2.3}$$

Where $A$and B are real Ginibre matrices. Real Ginibre matrices are nothing but matrices with all entries identically and independent distributed as a

Gaussian with average at zero and standard deviation equal to one. The imaginary part of the new matrix (2.3) is completely independent of the real part because $\mathrm{Re}\, G_{ij}$ depends of A_{ij} alone and on the other hand $\mathrm{Im}\, G_{ij}$ depends only on B_{ij}. Furthermore, the trace of $V(M)$ reads,

$$\mathrm{tr}M^2 = \sum_i M_{ii}^2 + 2\sum_{i<j} M_{ji}M_{ij} = \sum_i M_{ii}^2 + 2\sum_{i<j} |M_{ij}|^2 \quad , \tag{2.4}$$

Accordingly, the partition function is written as:

$$Z = \left(\prod_{i=1}^{N}\int_{-\infty}^{+\infty} dM_{ii}\, e^{-NM_{ii}^2}\right)\left(\prod_{i<j}\int_{-\infty}^{+\infty} dM_{ij} e^{-NM_{ij}^2}\right)\times$$
$$\left(\prod_{i<j}\int_{-\infty}^{+\infty} dM_{ji} e^{-NM_{ji}^2}\right) \quad , \tag{2.5}$$

Which can be reformulated as (due to the r.h.s of (2.4)):

$$\begin{aligned} Z &= \left(\prod_{i=1}^{N}\int_{-\infty}^{+\infty} dM_{ii}\, e^{-NM_{ii}^2}\right)\times\left(\prod_{i<j}^{N}\int_{-\infty}^{+\infty} dM_{ij}\, e^{-2N|M_{ij}|^2}\right) \quad , \\ &= \left(\int_{-\infty}^{+\infty} dM_{ii}\, e^{-NM_{ii}^2}\right)^N\left(\int_{-\infty}^{+\infty} dM_{ij} e^{-2NM_{ij}^2}\right)^{N(N-1)} \quad , \end{aligned} \tag{2.6}$$

It follows:

$$Z_{GUE} = \left(\frac{\pi}{N}\right)^{N/2}\left(\frac{\pi}{2N}\right)^{N(N-1)/2} = \left(\frac{\pi}{N}\right)^{N^2/2}\left(\frac{1}{2}\right)^{N(N-1)/2} \quad , \tag{2.7}$$

Where GUE stands for Gaussian unitary ensemble, here "unitary" stands for the unitary symmetry of the Hermitian matrices. For higher order potential the partition function does not factorize anymore and thus the elements are not independent anymore. General matrices with d entries are called Wigner matrices. Only the GUE is at the same time Wigner and unitary, while more complicated unitary matrices are not Wigner anymore. Due to this, we shall reformulate (2.1) and (2.2) in terms of eigenvalues of the matrix to be able to compute the partition function (see appendix A). The partition function given by the eigenvalues λ_i of a $N \times N$ Hermitian matrix reads:

$$Z = \frac{1}{N!(2\pi)^N}\prod_{i=1}^{N}\int d\lambda_i\, e^{-N\sum_i V(\lambda_i)}\prod_{1\le i<j\le N}|\lambda_j - \lambda_i|^2 \quad , \tag{2.8}$$

Here the constant decoupled of the integral is the volume of the unitary group (see [50, 55] for another derivation). In accord with appendix A, the Vandermonde's determinant equivalence is held only because of the power of two in (2.8). So far we have dealt only with the GUE ensemble, the oldest

to be known and arguably the simplest. The GUE ensemble has its unitary invariance as its main characteristic and is named after it. This invariance can be written as,

$$M = M^\dagger = U\Lambda U^\dagger \quad , \quad UU^\dagger = \mathbb{1}, \tag{2.9}$$

Here U denotes unitary matrices. Thus, we rewrite (2.8)

$$Z = \frac{1}{Vol(Group)} \prod_{i=1}^{N} \int d\lambda_i \, e^{-Nf(\lambda)} \prod_{1 \leq i < j \leq N} |\lambda_j - \lambda_i|^\beta \quad , \tag{2.10}$$

Where β is known as the Dyson's index, which in classical RMT admit three possible values: 1 for the GOE (orthogonal) and 4 for the GSE (symplectic) as well as 2 for the GUE. The GOE is composed by real symmetric matrices and the GSE is formed by real quaternion self-dual matrices. The probability distribution of the two ensembles are respectively invariant under a change

$$\begin{aligned} M &= O\Lambda O^T \quad , \quad OO^T = \mathbb{1} \quad , \\ M &= W^R \Lambda W \, , \quad WW^\dagger = \mathbb{1} \quad , \end{aligned} \tag{2.11}$$

Where W is a quaternion matrix. Alternatively we could have written W^R(Self-Dual) $= W^{-1} = W^T$(more details available here [55]). Note that the exponential in (2.1) is invariant under (2.9) due to cyclic permutation invariance of the trace. While one has to handle properties of orthogonal polynomials and determinants in GUE case, the alternative ensembles requires some extra level of machinery. This is so because we no longer are dealing with complex matrix elements, therefore the Pfaffians, skew-orthogonal polynomials as well as anti-symmetric scalar products become necessary tools. Briefly, one has to take the $\beta = 2$ case as the cornerstone and extend this to a determinant with quaternion elements, which require a cumbersome task of Pfaffian calculations[55]. A next natural step is the establishment of an analogy with physical systems to understand the role of the latter term in (2.8). Hereinafter:

$$Z = c_N \prod_{i=1}^{N} \int d\lambda_i \, e^{-N^2 S(\{\lambda_i\})} \quad ,$$

$$S(\{\lambda_i\}) \equiv \frac{1}{N} V_{eff} = \frac{1}{N} \sum_i V(\lambda_i) - \frac{\beta}{N^2} \sum_{i<j} \ln|\lambda_j - \lambda_i| \quad , \tag{2.12}$$

Here S stands for the action and V_{eff} is the effective potential . What apparently had no physical picture whatsoever (the definition (2.1)), now gained some physical panorama, namely: There is an interaction between all eigenvalues which in turn make each one be coupled to one another (repulsion of Coulomb character). It was soon realized by Wigner that the earlier version

of RMT could be strengthened if adopted the log-gas analogy, which was later developed in depth by Dyson [56].

Consider that this physical system is in thermodynamic equilibrium and existing in a two-dimensional setting. From statistical physics we also know that the probability density of the positions of the electric charges to be of order e^{-E/k_BT}, implying that the large-N limit actually corresponds to the limit of T approaching absolute zero. This means that the eigenvalues are confined in some restricted region, which in the case of a Gaussian potential would be the interval [-2,2] (In chapter four we explain how to obtain the interval). In other words, because of the repulsion, it is very implausible that the eigenvalues are either very close or too distant of each other. Moreover, there are different ways to compute the probability density of finding the eigenvalue λ among its neighbours, we will see two different ways to do so in the chapter four. For the sake of the analogy, one might carry on the calculation of the probability density. For instance, notice that a charged thin line has a potential of logarithmic character, and we have a pair interaction of the same type in (2.12). Furthermore, if we impose a conservation of charge in the system (stable), it is possible to find the celebrated Wigner's semi-circle law, which is:

$$\rho(\lambda) = \frac{1}{2\pi}\sqrt{4-\lambda^2} \quad . \tag{2.13}$$

As often one does in electrostatics, the overall potential due to all pair potential interactions is computed as,

$$V(\lambda) = \int_{-2}^{2} d\lambda' \ln|\lambda - \lambda'|\rho(\lambda') \quad , \tag{2.14}$$

We have assumed continuum distribution because we impose the N to be large, otherwise it would become a sum instead of an integral. The necessary calculation to find $V(\lambda)$ is not trivial (see [55, 57]), nonetheless, the last integral is calculated to be exactly $\frac{\lambda^2}{2}$, endorsing both the Wigner's semi-circle law and the relevance of the log-gas analogy.

Before an overview of the broad range of RMT applicability, let us first discuss its advantages, because at the end of the day, this is the reason why RMT is so successful. The first one is universality: In the large matrix dimension the correlations of the spectrum of an particular ensemble are independent of the probability distribution (2.1) that is used to define it, rather depending only in the invariance of the distribution. As one might expect, the correlations are also independent from the chosen couplings. Besides, RMT recover much of known effective field theories in this limit. Surprisingly, the large-N limit in RMT is related to the limit cases of another statistical ensembles, albeit they are not studied through random matrices.

Remarkably, the intrinsic universality property is expected to hold even without the invariance features of the ensembles. This most basic feature of RMT is argued to be the reason why Wigner paid attention to the Wishart matrices and applied it to nuclear physics in the early fifties [57]. In addition, RMT techniques allow analytical computations that are almost impossible to accomplish in its own formulation. As if this was not enough, RMT also admits additional symmetries (time reversal, chiral etc. [55, 57]), not to mention the possibility of couple it to external frameworks. RMT also have the possibility to be applied to fields that actually are not built upon the analysis of random matrices. Even though some of its applications are based on some ensembles that are not originated from random matrices, they indeed can be analysed by some general RMT techniques. Commonly, RMT is carried to tackle two kinds of issues: as a counting tool to resolve enumerative combinatorics (such as graphs, random surfaces, knots, folding problems, orbits, strings etc.) and as a random operator in order to analyse spectral properties of a given operator along with correlation functions (when it can not be treated explicitly). Roughly speaking, RMT can be thought as the overlap of linear algebra and probability theory, such that stochastic and random problems fit very well unto its techniques. After all, one could imagine that RMT might also have significant insights towards QCD. Either theoretical or phenomenological parts of QCD can be understood by RMT techniques [55, 57, 58, 59]. Because RMT has some different approaches within itself there are many applications in fields thought to be uncorrelated, such as RNA folding, information theory, business, financial markets as well as economic models, growth models, optics (classical and quantum), chaos or condensed matter physics.

2.2 Matrix models and fatgraphs

One of the beautiful applications of RMT is in the field of enumerative combinatorics, particularly in the task of counting graphs. In fact large-N matrix models do generate planar graphs which are very important to the discretization of surfaces in quantum gravity. This was inspired by the $1/N$ expansion in QCD [60], and their applications are not restricted to the problem of formulate a quantum theory of gravity. The key element in the combinatorics of the graphs relies on the Wick's Theorem, which enables us to compute graphs drawn on a Riemann surface. Consider the following integral:

$$\left\langle x^{2n} \right\rangle = \frac{\int_{-\infty}^{+\infty} dx\, x^{2n}\, e^{-\frac{x^2}{2}}}{\int_{-\infty}^{+\infty} dx\, e^{-\frac{x^2}{2}}} \quad . \tag{2.15}$$

Figure 2.1: Diagram corresponding to $\langle x_i x_j \rangle$.

The procedure to compute the above formula is quite simple. One rewrites the denominator of (2.15) plugging a constant γ alongside x^2, further obtaining a value of $\sqrt{\frac{2\pi}{\gamma}}$ for the integral. Hence, one has only to take successive derivatives of the given result relative to γ, yielding $(2n-1)!!$. A much more elegant way to compute (2.15) is the following:

$$\begin{aligned} \left\langle e^{px} \right\rangle &= \frac{1}{\sqrt{2\pi}} \int_{-\infty}^{+\infty} dx\, e^{-\frac{x^2}{2}+px} \quad , \\ &= \frac{1}{\sqrt{2\pi}} \int_{-\infty}^{+\infty} dx\, e^{-\frac{1}{2}\left((x-p)^2-p^2\right)} = e^{\frac{p^2}{2}} \quad . \end{aligned} \tag{2.16}$$

Observe that if we take the derivative twice and then set $p = 0$, we will achieve $\langle x^2 \rangle$. Analogously, if one takes $2n$ derivatives of $\left\langle e^{px} \right\rangle$ at $p = 0$, we once again find $(2n-1)!!$. This has a important interpretation. The idea here is that we are taking derivatives in pairs, which means that the factor $(2n-1)(2n-3)\cdots 1$ represents the number of possible pairs. Suppose we have $2n$ points that can be joined in pairs. The point p_{2n} can create $2n-1$ different pairs. After the first pair is made, the next point, have $2n$ minus two and minus one (representing itself) as the possible number of pairs, which is $2n-3$, and so on. In other words:

$$\left\langle x_{i_1} \cdots x_{i_n} \right\rangle = \sum_{pairs} \prod_{i \neq j}^{2n} \left\langle x_i x_j \right\rangle \quad , \quad \langle x_i x_j \rangle = \delta_{ij} \quad . \tag{2.17}$$

This is nothing but the Wick's theorem for scalars. Following the same procedure, we introduce the Wick's theorem for matrices. Again we consider an expectation value, now for $N \times N$ Hermitian matrices, as follows:

$$\left\langle \mathcal{A}(M) \right\rangle = \frac{\int dM\, e^{-N \mathrm{tr} \frac{M^2}{2}} \mathcal{A}(M)}{\int dM\, e^{-N \mathrm{tr} \frac{M^2}{2}}} \quad , \tag{2.18}$$

applying the same strategy, one finds (see appendix B for a derivation):

$$\left\langle M_{ij} M_{kl} \right\rangle = \frac{\partial}{\partial S_{kl}} \frac{\partial}{\partial S_{ij}} \left\langle e^{\mathrm{tr} SM} \right\rangle = \frac{1}{N} \delta_{ij} \delta_{kl} \quad , \tag{2.19}$$

Which yields,

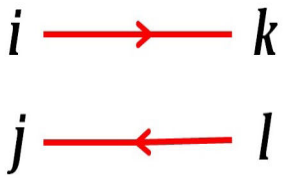

Figure 2.2: Diagram corresponding to $\langle M_{ij} M_{kl} \rangle$.

$$\left\langle M_{i_1 j_1} \cdots M_{i_{2n} j_{2n}} \right\rangle = \sum_{pairs} \prod_{\substack{i \neq k \\ j \neq l}}^{2n} \left\langle M_{ij} M_{kl} \right\rangle \quad . \tag{2.20}$$

Remarkably, we can link this with Feynman's diagrams. For instance, we now write down the partition function of the ϕ^4 field theory

$$Z = \int_{-\infty}^{+\infty} \frac{d\phi}{\sqrt{2\pi}} e^{-\frac{\phi^2}{2} + g\frac{\phi^4}{4!}} \quad , \tag{2.21}$$

Then we evaluate it in a perturbation series:

$$\sum_{n=0}^{+\infty} \frac{1}{n!} \int_{-\infty}^{+\infty} \frac{d\phi}{\sqrt{2\pi}} e^{-\frac{\phi^2}{2}} \left(g \frac{\phi^4}{4!} \right)^n = \sum_{n=0}^{+\infty} \frac{g^n}{n!} A_n \quad . \tag{2.22}$$

Observing that A_n is the $\langle \phi^{4n} \rangle$, we naturally see that its diagram must be a point vertex with four lines emerging from it (not oriented because there are not labels such as i or j). On the other hand, if we rather evaluate an integral substituting the scalar ϕ by a $N \times N$ Hermitian matrix M, we would have

$$A_n = \int dM \, e^{-N \mathrm{tr} \frac{M^2}{2}} M_{i_1 j_1} \cdots M_{i_4 j_4} \quad . \tag{2.23}$$

As we know, we can represent a sum over a product of matrices as a trace,

$$\mathrm{tr}(M^p) = \sum_{pairs} \prod M_{i_k j_k} \quad , \tag{2.24}$$

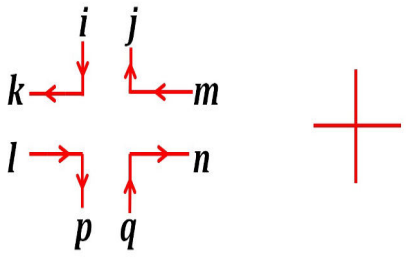

Figure 2.3: On the left we see the hermitian matrix four-point vertex, while on the right we see the scalar four-point vertex.

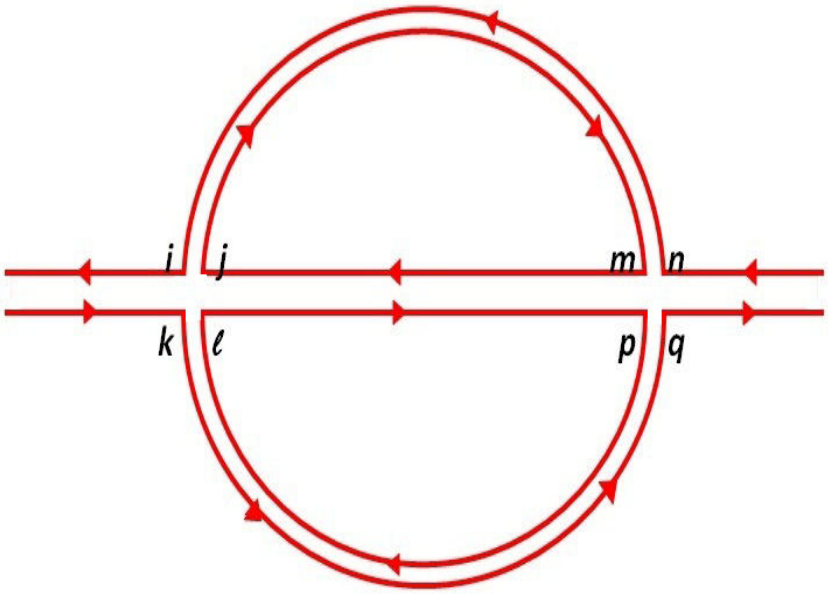

Figure 2.4: Double four-point vertex illustration. Each propagator (edge) contributes with a $1/N$ term whereas the closed loops (faces) and the vertices contribute with N.

Then, is natural to replace expectation values of matrices by the trace of matrices. Furthermore, the above relation means that the $\langle \mathrm{tr} M^p \rangle$ will generate a number of diagrams like those in figure 2.3 in which all of them converge, although not towards a point, creating a thick structure. This thick structure is important to form a two dimensional surface. In fact the diagrams without orientation and thin are not capable to establish a Riemann surface. What happens is that the oriented links form closed internal (oriented) loops (see figure 2.6) identifying the location and orientation of each face, explaining why one needs thick diagrams ('fatgraphs'). In the perturbative series of (2.22) the g^n counts the number of diagrams built up with n different four-point vertex. But as we want to study dynamical triangulations, we change our ansatz to

$$Z = \int dM\, e^{-N\left(\frac{\mathrm{tr}M^2}{2} - g\frac{\mathrm{tr}M^3}{3}\right)} \quad . \tag{2.25}$$

It is plain to see that this integral generates three-point vertex: Each edge of the diagram is dual to the edge of a triangle, the same for its faces and vertices, then we form a great number of connected three-point vertices that form closed oriented polygons. The dual of these polygons are nothing but triangles, as depicted in figure 2.6. We are able to make a connection between Feynman's rules and the hermitian matrix integral: For each hermitian matrix propagator we associate it to a factor of N^{-1} (recall that the propagator of the field theory is the inverse of the higher polynomial term in the potential), For each vertex a factor of N as well as for each face (closed loop). The argument

is that for each propagator the average (2.19) will give $1/N$ because of the deltas δ_{ij}, δ_{kl}. For the closed loops however, we have that the closed path will make $j = i$ and $k = l$, therefore we have a sum over the deltas δ_{ii}, δ_{kk}, which clearly gives a factor of N^2, then dividing by N we do obtain the overall N factor for the faces. For the vertices we can use the same argument (See figure 2.4). Now if we take the sum over the logarithm of all closed loops, the overall factor for a number V of vertices, F faces along with E edges is N^{F+V-E}. The power in N is well known as the Euler characteristic:

$$\chi = 2 - 2h \equiv V - E + F \quad , \tag{2.26}$$

Where h is the genus of the surface (number of holes on the surface). The physics of the described procedure is quite simple, we only computed the free energy as a sum over N to the power of the Euler characteristic. This in turn conceives what is called topological expansion:

$$F(t) = \sum_h N^{2-2h} F_h(t) \quad , \tag{2.27}$$

Where t is the 't Hooft parameter and is related to the size of the matrix as $t = g_s N$ (g_s is the string coupling). In the planar limit ($N \to +\infty$) we have instead,

$$\lim_{N\to+\infty} \frac{1}{N^2} F = F_0 \equiv F^{(sphere)} \quad . \tag{2.28}$$

Known as the 'sphere contribution' of the free energy. An interesting relation in [61] expands the sphere contribution of the free energy around the critical point of g for the m-th multi-critical region.:

$$F_0(g) \approx (g_c - g)^{2-\gamma} \sim \sum_n n^{\gamma-3} \left(\frac{g}{g_c}\right)^n \quad , \quad \gamma = -\frac{1}{m} \quad , \tag{2.29}$$

Here n is the number of vertices. Because the number of vertices is proportional to the area, when the coupling g approaches its critical value the area goes to infinity (remember that g^n counts the number of vertices), therefore in this regime we would have

$$F_0(g \to g_c) \sim A^{\gamma-3} \quad . \tag{2.30}$$

2.3 Euclidean quantum gravity

We already explained how matrix integrals generates fatgraphs (the importance of the type of matrix, whether hermitian or not, is related to the solutions of the matrix model). We shall now analyse how the gravitational action and partition function are inserted in this context. Foremost, we write down the action over a manifold $\mathcal{M}$ in a four dimensional theory of gravity,

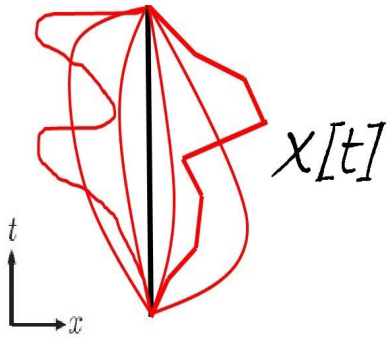

Figure 2.5: Sum over histories in quantum mechanics. In black is seen the shorter path, in red are depicted six different paths (or histories).

$$S = \frac{1}{16\pi G}\int_{\mathcal{M}} d^4x\,\sqrt{|det\,g_{ab}|}\,(R-2\mu) + \frac{1}{8\pi G}\int_{\partial\mathcal{M}} d^3x\,\sqrt{|\mathcal{H}|}\,\mathcal{K} \quad , \tag{2.31}$$

Where G denotes the Newton constant, g_{ab} the metric, R the scalar curvature and μ the cosmological constant. The second term of the r.h.s in (2.31) is the boundary term while the first term is the well known Einstein-Hilbert action, and $(\mathcal{H},\mathcal{K})$ are respectively determinant of the induced metric and the induced scalar curvature. We want to find an expression for the partition function in four dimensional quantum gravity. Recall that in quantum mechanics the partition function (transition amplitude) is expressed as

$$\mathcal{Z} = \int \mathcal{D}x \int \frac{\mathcal{D}p}{2\pi\hbar}\, e^{\frac{i}{\hbar}S} = const \times \int \mathcal{D}[x(t)]\, e^{\frac{i}{\hbar}S[x(t)]} \quad . \tag{2.32}$$

Thereby, we formulate the amplitude probability (partition function) over a path (from one geometry to another one) as

$$\mathcal{Z} = \int \mathcal{D}[g_{ab}] e^{\frac{i}{\hbar}S_{EH}[g_{ab}]} \quad . \tag{2.33}$$

Roughly speaking, if one considers the above partition function as the probability amplitude of a transition of spatial geometries and applies it to the schrdinger equation, the result is the WDW equation, in which time does not have any role whatsoever, preventing the equation to describe the time evolution of the universe [62]. Not only in this context, but generally, the definition in (2.33) causes many problems in quantum gravity. For instance, often in the realm of quantum mechanics the complex nature of the exponential in (2.32) is removed after a Wick's rotation ($\tau \to it$) without any conceptual or technical problems arising, connecting quantum mechanics to statistical mechanics. However, this lack of difficulties does not hold when a Wick's rotation is performed in a partition function over $\mathcal{D}[g_{ab}]$ [63]. The main issue here relies on the fact that such rotation in not diffeomorphism invariant. One of the best approaches to tackle the integration over $\mathcal{D}[g_{ab}]$ is Liouville gravity, which will

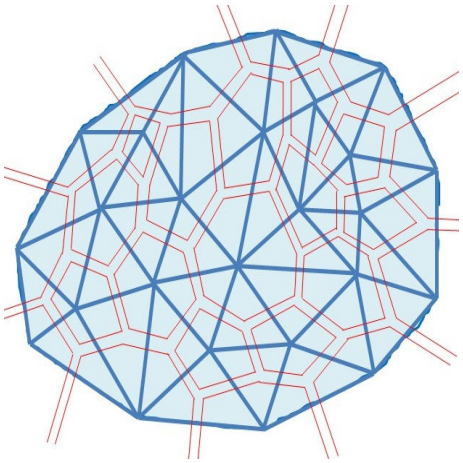

Figure 2.6: Random triangulation (blue) over a surface (light blue) and the dual graphs (red) of a three-point vertex of a Hermitian matrix model.

be shortly introduced in the next section. Yet, in Euclidean quantum gravity we have the provisional change from Lorentzian manifolds to Euclidean ones, and the partition function becomes

$$\mathcal{Z} = \int \mathcal{D}[g_{ab}] e^{-S[g_{ab}]} \quad . \tag{2.34}$$

Now, in two dimensions QG has an interesting particularity: it does not have degrees of freedom. The Gauss-Bonnet theorem is responsible for that. The theorem states,

$$\int_{\mathcal{M}} d^2x \sqrt{|det\, g_{ab}|} R = 4\pi\chi(h) \quad . \tag{2.35}$$

For instance, a naive integration of triangulated surfaces can be carried out to show that theorem holds. Of course the type of polygon does not interfere in the continuum limit results, yet we are mainly interested in triangulations here. We want to make a shift of paradigm, precisely:

$$\int \sqrt{|det\, g_{ab}|} R \rightarrow \sum_{Triangulations} \quad . \tag{2.36}$$

We start with very simple triangulations: Equilateral triangles turns the task of identifying the geometry of a closed loop dual to the triangulation easier. For example, if we impose that a group of six triangles form a planar hexagon (i.e zero curvature), the simple manoeuvre of removing or adding a triangle turns the surface such that it is no longer flat. The discrete scalar curvature for a given vertex i is then,

$$R_i = 2\pi \frac{(6 - N_i)}{V_i} \quad , \tag{2.37}$$

Where V_i is the volume associated to the vertex i. In figure 2.6 one observes that there are vertices linked to three, four, five, six or seven triangles,

recovering in some extent the continuum curvature of the real surface, because the more the number of triangles better we imitate the curvature of the surface in a given point. Note that the area of the surface is an integration over $\sqrt{|det\, g_{ab}|}$ (in two dimensions), and its discrete counterpart when summed should give the number of triangles, as each triangle has unit area, the counterpart should be $V_i = N_i$. Using topological relations (the number of edges is equal to the half of the sum of all triangles and the number of faces is equal to two thirds of the number of edges), we obtain:

$$\int d^2x\sqrt{|det\, g_{ab}|}R \to \sum_i \frac{V_i}{3}\frac{(6-N_i)}{V_i}2\pi = 4\pi\chi \quad , \tag{2.38}$$

Notice that the factor 1/3 comes from the fact that each triangle has three vertices and are counted three times. The theorem allows us to rewrite (2.32), in the following manner:

$$\mathcal{Z} = \int \mathcal{D}[g_{ab}]e^{-\frac{1}{16\pi G}\int d^2x\,\sqrt{|det\, g_{ab}|}\,(R-2\mu)} = \int \mathcal{D}[g_{ab}]\, e^{-\frac{\chi(h)}{4G}}\, e^{\frac{\lambda V_g}{8\pi G}} \quad ,$$

$$V_g = \int d^2x\sqrt{|det\, g_{ab}|} \quad , \tag{2.39}$$

And after a rescaling of constants, it yields a topological expansion:

$$\mathcal{Z} = \sum_{h=0}^{+\infty} e^{-\frac{\chi(h)}{G}}\, \mathcal{Z}_h \quad , \quad \chi(h) = 2-2h-b \quad , \tag{2.40}$$

b being the number of boundaries. Is important to realize that partition function of the gravitational action and the one of the matrix models are not the same. From the point of view of matrix models, the topological expansion is connected to the gravitational partition function in the following manner:

$$\mathcal{Z} \equiv \frac{\ln Z(g,N)}{\ln Z(0,N)} = \frac{F}{F_{Gaussian}} \quad . \tag{2.41}$$

The gravitational partition function of a fixed genus h reads:

$$\mathcal{Z}_h = \int \mathcal{D}[g_{ab}]\, e^{-S(\mu,g)} = \int \mathcal{D}[g_{ab}]e^{-\mu V_g} \quad . \tag{2.42}$$

Now we shall use its Laplace transform:

$$\mathcal{Z}(V) = \int_0^{+\infty} d\mu\, e^{\mu V}\, \mathcal{Z}(\mu), \tag{2.43}$$

Thus:

$$\mathcal{Z}(V) = \int_0^{+\infty} d\mu \Big(\int \mathcal{D}[g_{ab}]e^{-\mu V_g} \Big) e^{\mu V} = \int \mathcal{D}[g_{ab}]\, \delta(V - V_g) \tag{2.44}$$

The above formula is the partition function for fixed volume. Well, one might wish to add boundaries, and in this case we make a change in the action:

$$S(\mu, \eta_i) = \mu V_g + \sum_i \eta_i L_i(g) \quad , \tag{2.45}$$

Here η_i represents the i-th boundary cosmological constant, while L_i the i-th boundary loop. In analogy with the above usage of Laplace's transform, we shall find the partitions function for either fixed boundary loops or boundary cosmological constants. It follows:

$$\mathcal{W}(\mu, \eta_1, ..., \eta_p) = \int \mathcal{D}[g_{ab}]\, e^{-\mu V_g} \prod_{i=1}^{p} e^{-\eta_i L_i(g)}, \tag{2.46}$$

Where p is the number of boundaries. Now using their Laplace's transform:

$$\mathcal{W}(\mu, L_i) = \prod_i \int_0^{+\infty} d\eta_i\, e^{\eta_i L_i} \left[\int \mathcal{D}[g_{ab}]\, e^{-\mu V_g} \prod_{i=1}^{p} e^{-\eta_i L_i(g)} \right] \tag{2.47}$$

We therefore arrive at what is known as the Hartle-Hawking wavefunctions:

$$\mathcal{W}(\mu, L_i) = \int \mathcal{D}[g_{ab}]\, e^{-\mu V_g} \prod_i \delta\big(L_i - L_i(g)\big) \quad . \tag{2.48}$$

2.4 Liouville theory

There are some continuum methods capable to handle the integral in (2.33). Broadly, all attempts to compute the partition function in two dimensions in a Minkowskian signature are derived from dilaton gravity. The general action is formulated as,

$$S_{2D} = const \times \int d^2x \sqrt{|g(x)|} \left[RX + U(X)(\nabla X)^2 - 2V(X) \right] \quad , \tag{2.49}$$

Depending on the scalar field X, where R is the scalar curvature and we see two potentials which defines any model of continuum two-dimensional gravity. For a list containing such models see [64, 65]. One of the most prominent among these models is the Liouville gravity. One generally starts with the the Polyakov action:

$$S(g, X^\sigma) = const \times \int d^2x \sqrt{|g|} \big(g^{ab} \partial_a X^\sigma \partial_b X^\sigma + \mu \big) \quad , \tag{2.50}$$

Which is an action similar to the relativistic free particle. The Polyakov action is a sophisticated manner to rewrite the Nambu-Goto action [66], in the same way there are different manners to write the action of the free particle. The evaluation of gravitational path integral is done through fixing a conformal gauge $g = e^{\gamma\phi}\hat{g}$, where γ is a parameter and ϕ is the Liouville field. Upon this procedure, one constructs the classical Liouville action [67]:

$$S_{CL} = const \times \int d^2x\sqrt{|\hat{g}|}\big(\hat{g}^{ab}\partial_a\phi\partial_b\phi + \frac{2}{\gamma}R\phi + \frac{\mu}{\gamma^2}e^{\gamma\phi}\big) \quad , \tag{2.51}$$

Which is Weyl invariant ($\phi \to \phi - \frac{a}{\gamma}$), making it a classical conformal field theory. Using apropriate quantization techniques [67, 68], the quantum Liouville action becomes,

$$S_L = const \times \int d^2x\sqrt{|\hat{g}|}\big(\hat{g}^{ab}\partial_a\phi\partial_b\phi + QR\phi + 4\pi\mu e^{\gamma\phi}\big) \quad . \tag{2.52}$$

This action is supposed to satisfy Virasoro algebra as well as conformal invariance, which impose the value for Q and for the central charge, namely:

$$Q = \frac{2}{\gamma} + \gamma \quad ; \quad c = 1 + 3Q^2 \quad . \tag{2.53}$$

After requiring BRST invariance in the effective action, two conditions arise:

$$Q = \sqrt{\frac{25-D}{3}} \quad ; \quad \gamma = -\frac{Q}{2} + \sqrt{\frac{1-D}{12}} \quad . \tag{2.54}$$

We therefore can extract critical exponents from Liouville gravity. For instance, we write down the partition function for fixed volume (similar to (2.44)) in the Liouville paradigm,

$$\mathcal{Z}(A) = \int \mathcal{D}\phi\mathcal{D}X e^{-S_{eff}}\delta(A_{\hat{g}} - A) \quad , \quad A_{\hat{g}} \equiv \int d^2x\sqrt{|\hat{g}|}\, e^{\gamma\phi}\,. \tag{2.55}$$

However if we make a shift $\phi \to \phi + \frac{a}{\gamma}$, where a is a constant, the fixed partition function for genus zero develops a critical behavior [51]:

$$\mathcal{Z}(\mathcal{A}) \sim A^{\Gamma_* - 3} \quad , \tag{2.56}$$

Where Γ_* is the string susceptibility. Keeping in mind (2.30), we obtain from (2.53), (2.54) and (2.56):

$$\Gamma_* = \frac{1}{12}\big(D - 1 - \sqrt{(D-25)(D-1)}\big) = -\frac{1}{m} \quad . \tag{2.57}$$

If $D = 0$ (target space) then $\gamma = \frac{1}{2}$ (only one critical region), corresponding to pure two dimensional gravity.

3
Discrete quantum gravity

In this chapter we present dynamical triangulation as a regularization of the Euclidean gravitational path integral (2.33). Following the special behaviour of two dimensional quantum gravity due to Gauss-Bonnet theorem, two dimensional DT admits analytical solutions and we see in particular how to obtain the Hartle-Hawking function within this context. However, a mayor problem with DT is its pathological behaviour when extending the model to higher dimensions. An attempt to address this problem is the introduction of CDT. The main arguments of this chapter follows [39].

3.1
Dynamical triangulations

In DT the main idea is to define the integral over geometries to a sum over triangulations. This was inspired by early work of Regge [69]. In this early work its shown that one can define curvature as piecewise linear combinations of simplices. Curvature is then located at the vertices. In this way we formulate the Gaussian curvature at the vertex v:

$$R_v = \frac{2\pi - \sum_v \theta_v}{V_v} = \frac{\epsilon_v}{V_v} \quad , \tag{3.1}$$

where ϵ_v is the deficit angle and V_v the volume associated to the vertex (which is defined through the volume of the dual lattice). Therefore, we find that the Regge's action is

$$S_{Regge} = \sum_v (\mu V_v - G\epsilon_v) \quad . \tag{3.2}$$

We define the gravitational path integral through,

$$\mathcal{Z} = \int \mathcal{D}[g_{ab}]\, e^{-S[g_{ab}]} \;\rightarrow\; \sum_T \frac{1}{C_T}\, e^{-S_{Regge}(T)} \quad , \tag{3.3}$$

Here C_T is the dimension of the automorphism group of the triangulation T. We replace the former action by,

$$S(\mu', \eta'_1, ..., \eta'_p) = a^2 \mu' N_{triangles} + a \sum_{i=1}^{p} \eta'_i l_i \quad , \quad S_T = a\mu' N_{triangles}. \tag{3.4}$$

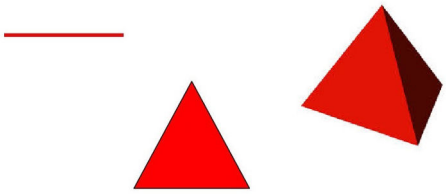

Figure 3.1: Building blocks of DT. In one dimension the simplex is a line, in two dimensions is a triangle while for three dimensions it is a tetrahedron.

Notice the prime notation, this is introduced to denote the discrete counterpart of (2.45). In analogy with the continuum formulation, we can define a expression for the loop equation:

$$\mathcal{W}(\mu', \eta'_1, ..., \eta'_p) = \sum_{l_i} \mathcal{W}(\mu', l_1, ..., l_p)\, e^{-a\sum_i \eta'_i l_i} \quad ,$$

$$\mathcal{W}(\mu', l_1, ..., l_p) = \sum_k e^{-a^2\mu' k}\, w_{k,l_i} \quad , \tag{3.5}$$

Here the $\mathcal{W}(\mu', \eta'_1, ..., \eta'_p)$ is a generating function of w_{k,l_i} (where k is the number of triangles and l_i the number of boundary edges). This turns the task of computing the two dimensional partition function of quantum gravity into a combinatorial problem of finding the number of triangulations, for a particular number of triangles and boundary components. For the sake of simplicity, we focus on a single boundary component and write:

$$\mathcal{W}(g, z) = \sum_k \sum_l g^k\, z^{-l-1}\, w_{k,l} \quad , \tag{3.6}$$

Where we identify $g = e^{-a^2\mu'}$ as the fugacity of the triangle and $z = e^{a\eta'}$. Henceforth we point out the difference between the generating functions for restricted and unrestricted triangulations, respectively:

$$\widetilde{\mathcal{W}}(g, z) = \sum_{k=1}^{+\infty} \sum_{l=3}^{+\infty} g^k\, z^{-l-1}\, w_{k,l} = \sum_{l=3}^{+\infty} \tilde{w}_l(g)\, z^{-l-1} \quad ,$$

$$\mathcal{W}(g, z) = \sum_{k=0}^{+\infty} \sum_{l=0}^{+\infty} g^k\, z^{-l-1}\, w_{k,l} = \sum_{l=0}^{+\infty} w_l(g)\, z^{-l-1} \quad . \tag{3.7}$$

For restricted triangulations, lines and points are not allowed. For unrestricted triangulations the least object is a point, then $k = 0$ and $l = 0$. Because we have included points in the generating function, the first term comes with z^{-1}, therefore $w_0(g) = 1$. In order to better understand the implications of these generating functions, let us see the expansion for restricted triangulations:

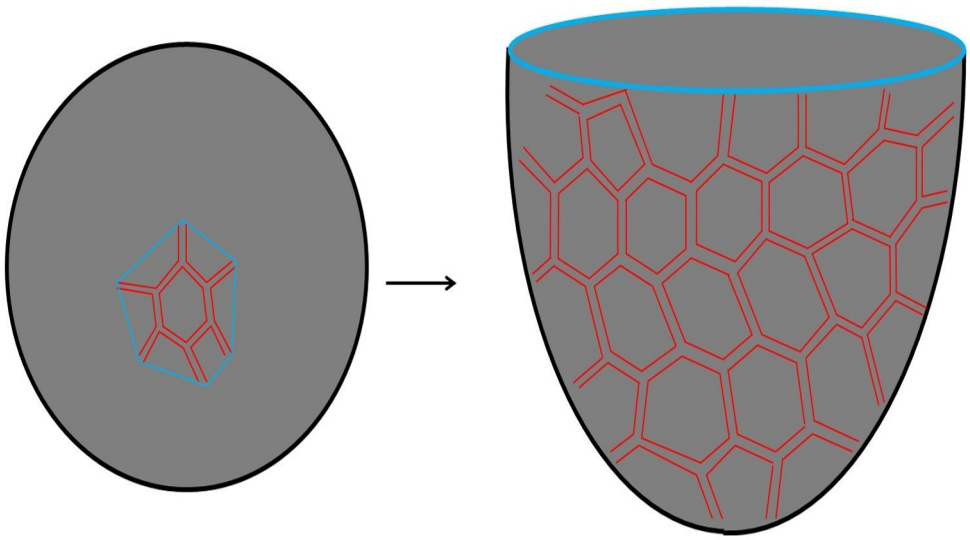

Figure 3.2: An example of triangulation over a surface. We remove a l-gon of the (say a sphere) and we end up with the disc function with a triangulation all over its surface (the blue circumference qualitatively represents the polygon removed.

$$\tilde{w}_l(g) = \sum_{k=3}^{+\infty} \tilde{w}_{k,l}\, g^k = \tilde{w}_{0,l} + \tilde{w}_{1,l}\, g + \tilde{w}_{2,l}\, g^2 + \cdots \tag{3.8}$$

Then we conclude that each triangle is coupled with a g and k triangles coupled with g^k. If we remove a triangle from the whole triangulation turns out that now we will have a term g^{k-1}. We want to create a connection between the Hartle-Hawking wavefunctions and the generating function in (3.6). In figure 3.2 we see a removal of a l-gon (A bunch of fatgraphs dual to a triangulation, see figure 2.6) and the result of this process is a disc function. The blue circumference is the same l-gon and it is associated with M^l (l edges). Now the generating function of this process can be written as (recall that the expectation value of the trace of M^k generates fatgraphs with k-point vertices):

$$\omega(z) = \sum_l w(\mu', g, l)\, z^{-l-1} = \frac{1}{N} \sum_l \langle \mathrm{tr} M^l \rangle z^{-l-1} \quad . \tag{3.9}$$

Using some trace properties, we rewrite it:

$$\begin{aligned} \omega(z) &= \frac{1}{N} \Big\langle \mathrm{tr} \Big[\sum_l M^l z^{-l-1} \Big] \Big\rangle = \frac{1}{N} \Big\langle \mathrm{tr} \Big[\frac{1}{z} \sum_l \Big(\frac{M}{Z} \Big)^l \Big] \Big\rangle \\ &= \frac{1}{N} \Big\langle \mathrm{tr} \frac{1}{z - M} \Big\rangle \quad . \end{aligned} \tag{3.10}$$

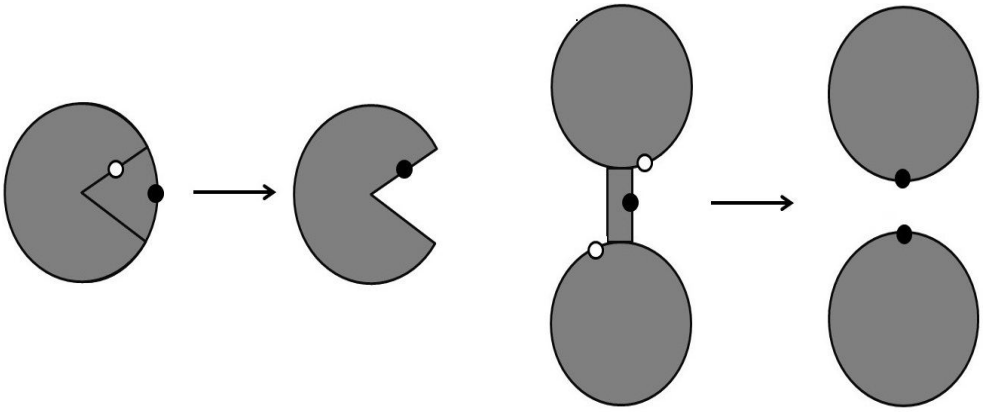

Figure 3.3: Possible decomposition moves in DT and its outcomes: On the left a black dot is a mark of the triangulation before a triangle is removed, a white dot is the mark after the removal, On the right a black dot is a mark of the triangulation before the link (between two disc functions) is removed and the white dot are the marks after the removal of the link.

In fact this is called resolvent and we will see in chapter four that the resolvent of the DT/CDT potentials matches exactly the generating function of the loop equation of the disc function in figure 3.2. For simplicity, henceforth we will not draw the triangulation but only a grey circle. Now, let us come back to the process of removal of a triangle concerned with the edges: We see in figure 3.3 that whenever removing a triangle we remove also a boundary edge ($l \to l-1$). But there are now two new internal boundary edges, such that at the end we have added one boundary edge to the original number of boundary edges. Let be x another variable such that $x \equiv z^{-1}$. Moreover, we rewrite (3.7) as:

$$\mathcal{W}(g,z) = \frac{1}{z}\sum_k \sum_l w_{k,l}\, g^k z^{-l} \quad , \tag{3.11}$$

As a result, we can define:

$$W(g,x) = z\mathcal{W}(g,z) = \sum_k \sum_l w_{k,l}\, g^k z^{-l} = \sum_k \sum_l w_{k,l}\, g^k x^l \, . \tag{3.12}$$

A general unrestricted triangulation, like a ball with a mark, is associated with $W(g,x)$. If we remove the mark, it will be associated with $W(g,x)-1$. Removing the triangle yields:

$$W_{(N-1)}(g,x) = \Big(W_{(N)}(g,x) - 1\Big) - x w_1(g) \ , \ W_{(N)}(g,x) \equiv W(g,x) \, , \tag{3.13}$$

Here (N) denotes the number of triangles of the generating function. Observing the expansion of $W(g,x)$, we find another way to express the removal of the triangle (recall that when one triangle is removed the total number of boundary edges is increased by one):

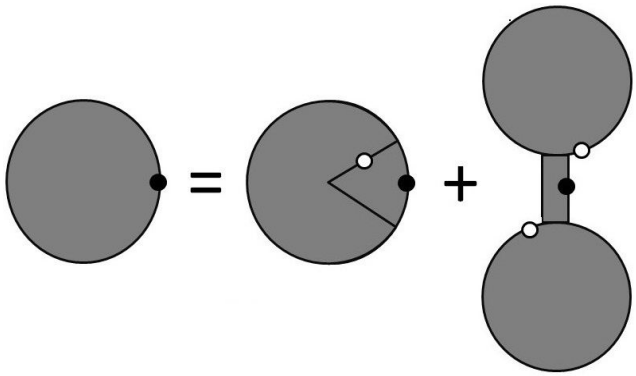

Figure 3.4: Graphic representation of the loop equation of the disc function.

$$W_{(N-1)}(g,x) = \sum_k \sum_l w_{k-1,l+1}\, g^{k-1} x^{l+1} = \frac{x}{g}\, W_{(N)}(g,x) \quad , \tag{3.14}$$

Now, because (3.13) and (3.14) represent the same removal of one triangle, we conclude:

$$W_{(N)}(g,x) \to \frac{g}{x}\Big[W_{(N)}(g,x) - x w_1(g) - 1\Big] \quad . \tag{3.15}$$

The next step is to figure out an expression for the removal of the double-link in figure 3.3. While removing a triangle we increase the initial number of edges by one, if one removes the double-link the outcome is the loss of two boundary edges. For each link removed there is a x multiplying the generating function, so, the expression correspondent to the figure 3.3 is:

$$W(g,x) \to 1 + x^2 W^2(g,x) \quad . \tag{3.16}$$

Applying the above expressions to the graphical representation we obtain:

$$W(g,x) = \frac{g}{x}\Big(W(g,x) - x w_1(g) - 1\Big) + 1 + x^2 W^2(g,x) \quad , \tag{3.17}$$

With the help of (3.11), one finds:

$$(z - g z^2)\mathcal{W}(g,z) = \Big[1 - g\Big(w_1(g) + z\Big)\Big] + \mathcal{W}^2(g,z) \quad . \tag{3.18}$$

By means of this, the solution reads,

$$\mathcal{W}(g,z) = \frac{1}{2}\Big[V'(z) - \sqrt{(V'(z))^2 - 4P(z)}\Big] \quad ,$$

$$V'(z) = z - g z^2 \quad , \quad P(z) = 1 - g\Big(w_1(g) + z\Big) . \tag{3.19}$$

The sign of the square root shall be chosen based on the asymptotic form of the generating function. For large z the generating function is required to be $\mathcal{W}(g,z) \sim 1/z$, then it explains why we chose the minus sign. If we take

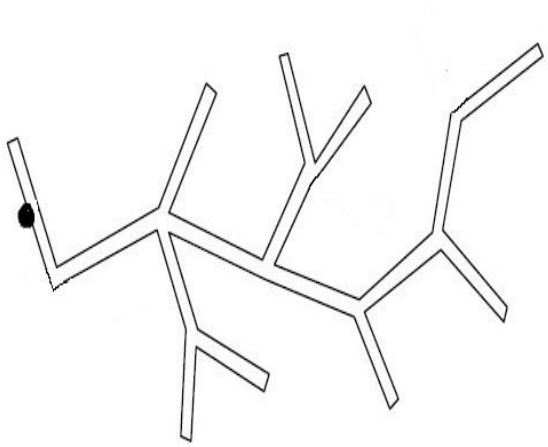

Figure 3.5: A rooted branched polymer.

the limit of g going to zero we would have a rooted branched polymer type of structure, as shown in figure 3.5. A consequence of taking $g = 0$ is:

$$\mathcal{W}(0,z) = \frac{1}{2}\left(z - \sqrt{z^2-4}\right) \quad . \tag{3.20}$$

The square root in the above formula gives rise to a branch cut in [-2,2]. We can generalize the form inside the square root as:

$$\left(V'(z)\right)^2 - 4P(z) = \left(gz - c(g)\right)^2 \left(z - c_+(g)\right)\left(z - c_-(g)\right) \quad , \tag{3.21}$$

When g is equal to zero we require:

$$c(0) = 1 \quad ; \quad c_+(0) = 2 \quad ; \quad c_-(0) = -2 \quad . \tag{3.22}$$

Once known the potential and the conditions that restrict the possible solutions, one is able to find the four unknown quantities: $w_1(g)$, $c(g)$, $c_+(g)$ and $c_-(g)$. We shall find these quantities for a DT potential plugging it unto (3.19), leading to a system of four equations with four unknown variables. Solving the system for c gives:

$$4c^3 - 6c^2 + 2c + 4g^2 = 0\,. \tag{3.23}$$

Among the three solutions, the only one which satisfies (3.22) reads:

$$c(g) = \frac{1}{2}\left(1 + \sqrt[3]{\frac{1}{3a}} + \sqrt[3]{\frac{a}{9}}\right) \quad ,$$

$$a = -36g^2 + \sqrt{3}\sqrt{432g^4 - 1}\,. \tag{3.24}$$

Once $c(g)$ is known, is straightforward to find the remaining unknown quantities in terms of the latter. For the support $[c_+, c_-]$, one can show, from the

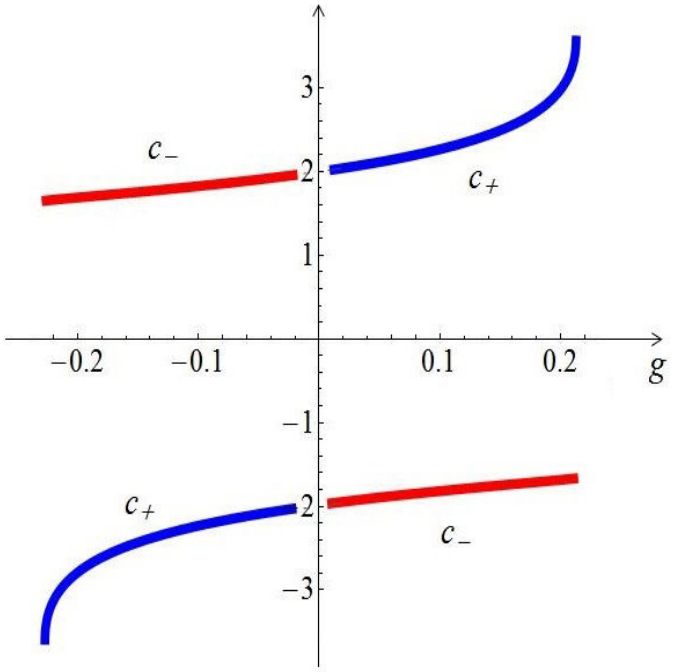

Figure 3.6: The function in blue is a representation of $c_+(g)$ and the one in red corresponding to $c_-(g)$.

system of equations, that they can be expressed as:

$$c_\pm(g) = \frac{1}{g}\left[\big(1-c(g)\big) \pm \sqrt{2c(g)\big(1-c(g)\big)}\right]. \tag{3.25}$$

3.2 Continuum limit of DT

The continuum limit is associated with the asymptotic form of w_{k,l_i} in (3.7) when both the number of triangles and edges (boundaries) approach infinity, while the cut-off a (edge of each triangle) approaches zero, in such a way that the product of the cut-off and the number of edges remains fixed. We want to know the exact form for the Hartle-Hawking wavefunction (2.46), (2.48). Due to the dimensions of μ' (bare cosmological constant) and η'_i (bare boundary cosmological constant), respectively $1/a^2$ and $1/a$, we have an additive renormalization:

$$\mu' = \frac{\mu'_c}{a^2} + \mu \quad ; \quad \eta' = \frac{\eta'_c}{a} + \eta \quad . \tag{3.26}$$

The critical points are:

$$g_c = e^{-\mu'_c} \quad ; \quad z_c = e^{-\eta'_c} \quad . \tag{3.27}$$

It follows:

$$g = e^{-a^2\mu'} = g_c\, e^{-a^2\mu} \quad ; \quad z = e^{a\eta'} = z_c\, e^{a\eta} \quad . \tag{3.28}$$

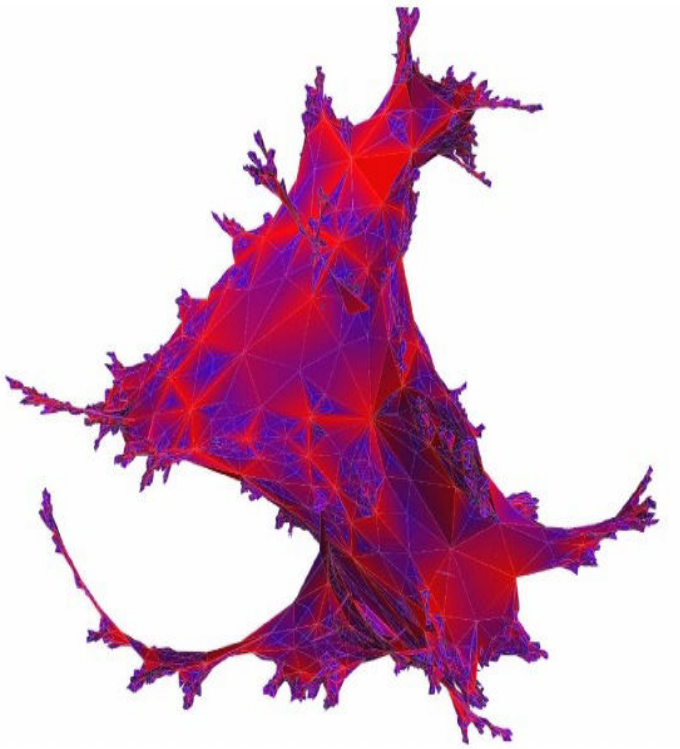

Figure 3.7: An example of quantum geometry in DT [70]. There are two colors which identify positive and negative curvature (respectively blue and red) according to equations (2.37) and (3.1).

Bearing in mind the radius of convergence of the analytic structure in this limit, we know that $z_c = c_+(g_c) = -c_-(g_c)$. Furthermore, one is able to find g_c as the radius of convergence of $w_1(g)$ (This value is $432^{-1/4}$ which agrees with (D.7)). Nevertheless, the important task here requires us to insert the scaling relations (3.28) into the resolvent (3.19) [71], finding:

$$\mathcal{W}(z) \sim a^{3/2}(\mu - \frac{\sqrt{\eta}}{2})\sqrt{(\mu + \sqrt{\eta})} \quad , \tag{3.29}$$

and

$$\mathcal{W}(\mu, \eta) = (\mu - \frac{\sqrt{\eta}}{2})\sqrt{(\mu + \sqrt{\eta})} \quad . \tag{3.30}$$

Using (2.47) we obtain:

$$\mathcal{W}(\mu, L) = L^{-\frac{5}{2}}(1 + \sqrt{\mu}L)e^{-\sqrt{\mu}L} \quad . \tag{3.31}$$

3.3 Causal dynamical triangulations

In the same way that DT is associated to Euclidean quantum gravity CDT is associated to Lorentzian quantum gravity. Although is true that DT does not bring expected well-behaved quantum geometries, even if it was not so, CDT is still necessary to recover the background geometry (general relativity). In CDT the triangulation is created with Minkowskian simplices instead of euclidean

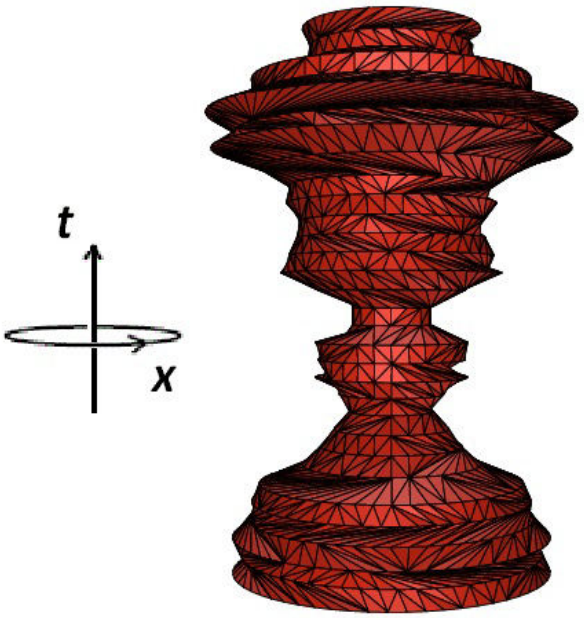

Figure 3.8: An example of spacetime in CDT [41]. This is an analogue of figure 2.4.

in DT, where these triangles have one spacelike edge (horizontal) and the two remaining edges are timelike (see figure 6.1 in [39]), and one constructs a triangulation with t time slices of size equal to one. Because the structure glues together spacelike with spacelike only and timelike with timelike only as well, causality is present in the whole structure. One can perform a Wick's rotation on the timelike edges and we would have

$$e^{iS^{(l)}_{Regge}} \rightarrow e^{-S^{(e)}_{Regge}} \quad , \tag{3.32}$$

Here l stands for Lorentzian and e for Euclidean. The action for CDT has the same structure as in (3.4). Particularly, we can compute the one-step propagator [40]:

$$G_{\mu'}(l_2, l_1, t) = \sum_{\mathcal{T}(l_1,l_2,t)} \frac{1}{C_T} e^{-a^2\mu' N_{Triangles}} \quad , \tag{3.33}$$

Where l_1 denotes the initial boundary edge and l_2 the final one of the triangulation and C_T has the same meaning as in (3.4) but $\mathcal{T}$ denotes the causal triangulations with such initial and final boundary lengths in a structure with t time-slices. As for DT, we present a generating function, namely:

$$G_{\mu'}(x, y, t) = \sum_{k,l} x^k y^l G_{k,l,t} \quad , \tag{3.34}$$

Where again the x, y are related to the boundary cosmological constants as $x = e^{-a\mu'_i}$, $y = e^{-a\mu'_0}$. One can show that the generating function is expressed

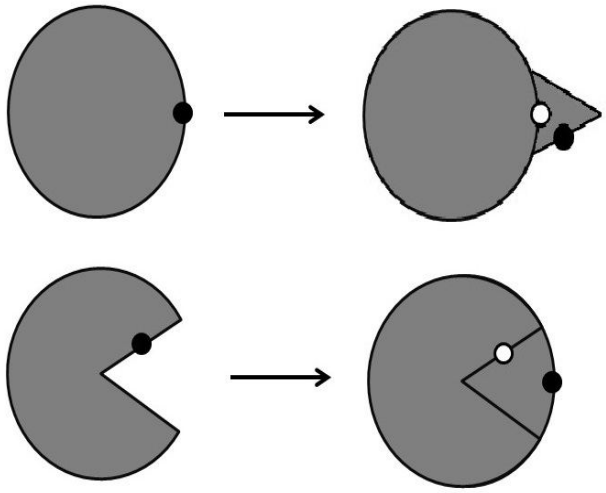

Figure 3.9: Decomposition moves for CDT: The moves consists of adding a triangle, whereas the white dot shows the mark before the addition of the triangle, and the black one the mark after the triangle was added.

[39, 40]:

$$\begin{aligned} G(x,y,g,1) &= \sum_{k=1}^{+\infty} \frac{1}{k}\left(\frac{gx}{1-gx}\frac{gy}{1-gy}\right)^k \\ &= -\log\left[1-\frac{g^2xy}{(1-gx)(1-gy)}\right] \quad , \end{aligned} \tag{3.35}$$

Where a factor of gx is assigned for triangles pointing up (in the time slicing) and a factor of gy to one pointing down (alternatively, gx is assigned to the spacelike edge on the initial boundary length and gy to the final boundary length). This coupling g is the equivalent of the one in (3.6), i.e the fugacity of the triangle. Now, because in the first section of this chapter we studied DT through the loop equations, relating the generating function with the resolvent, we shall do the same in this section as well. It is remarkable that for both types of triangulations, there are loop equations and matrix models which describes the physics of the theory. Following the steps of section 3.1, we briefly summarize the loop equations of CDT. Causal triangulations can be generated by adding triangles, with two possible models (figure 3.9) [39, 72]: gluing two edges of the additional triangle unto the triangulation, one mark to the edge in the loop circumference and the remaining mark to the next edge (in the clockwise direction) or adding a triangle using the method of gluing one of its edges to the marked edge of the triangulation assigning the new mark to the new edge (again clockwise direction). If the two moves are done together, we have the CDT equivalent of (3.17), as depicted in figure 3.10:

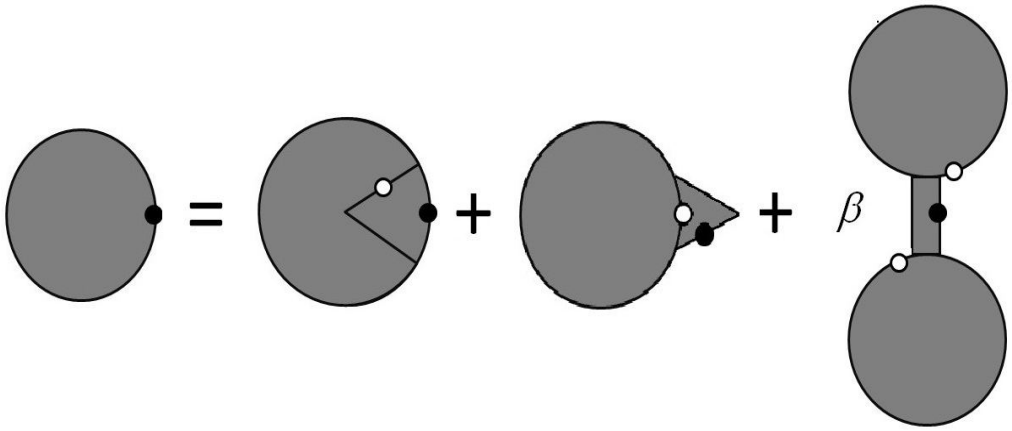

Figure 3.10: Representation of the loop equation of the disc function in generalized CDT.

$$\mathcal{W}_\beta(g,x) = \frac{g}{x}\Big\{\mathcal{W}_\beta(g,x) - xw_1(g) - 1\Big\} + 1 + \beta x^2 \mathcal{W}_\beta^2(g,x) + gx\mathcal{W}_\beta \quad , \tag{3.36}$$

Here the β factor is related to the inclusion of spatial topology change [72], and (3.36) is known as generalized CDT loop equation. It follows (here we apply the same reasoning for DT):

$$\mathcal{W}_\beta(g,z) = \frac{1}{2\beta}\left(V'(z) - \sqrt{(V'(z))^2 - 4\beta P_\beta(z)}\right) \quad ,$$

$$V'(z) = -g + z - gz^2 \quad , \quad P_\beta(z) = 1 - g\Big(w_1(g,\beta) + z\Big) \, . \tag{3.37}$$

Notice that the role of β here is similar to the t in chapter four. Applying the CDT potential to (3.21) we obtain:

$$2c^3 - 3c^2 + (1+2g^2)c + (2\beta - 1)g^2 = 0 \quad . \tag{3.38}$$

This leaves us with,

$$c(g) = \frac{1}{2}\left[1 + (1-4g^2)\sqrt[3]{\frac{2}{\alpha'}} + \frac{1}{3}\sqrt[3]{\frac{\alpha'}{2}}\right] \quad ,$$

$$\alpha' = -216g^2\beta + \sqrt{46656g^4\beta^2 + 4(3-12g^2)^3} \quad , \tag{3.39}$$

alongside with

$$c_\pm(g) = \frac{1}{g}\left(1 - c \pm \sqrt{2}\sqrt{(1-c)c - g^2}\right) \quad . \tag{3.40}$$

Figure 3.11 shows the plot of the support as a function of g and β. For the scenario when β vanishes the cut vanishes as well, corresponding to the pure CDT case when topology changes are not allowed, we also notice that for bigger

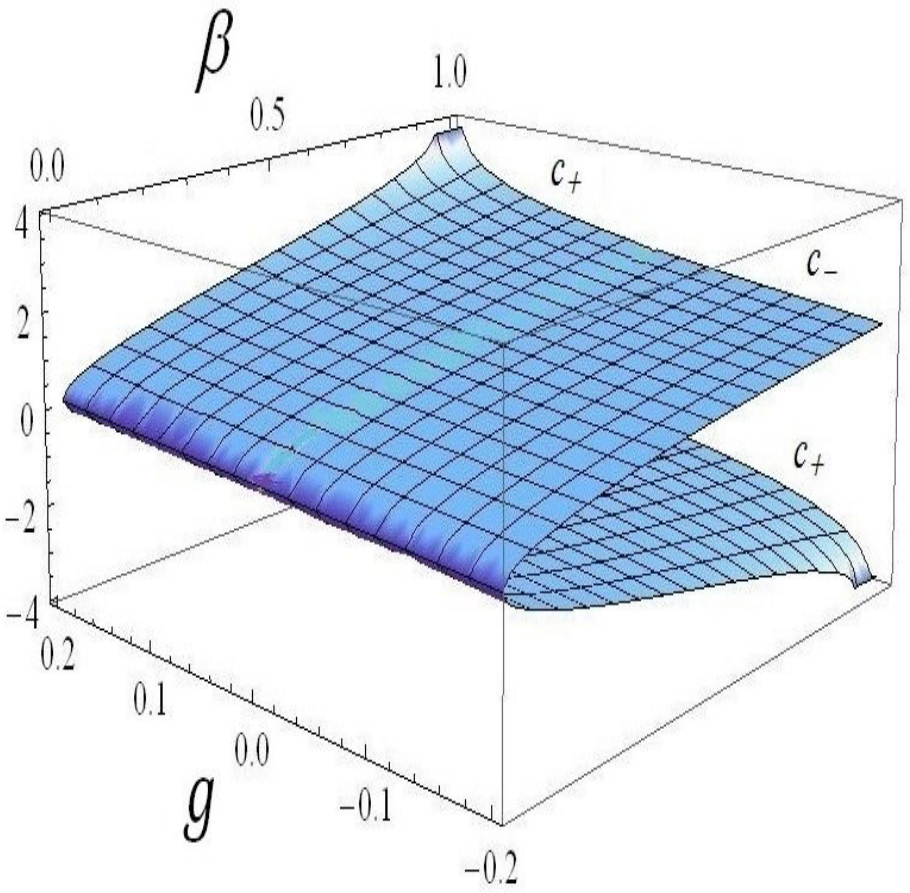

Figure 3.11: The CDT analogue of figure 3.6. In the pure CDT realm ($\beta = 0$) both $c_+(g)$ and $c_-(g)$ vanish.

values of β its behaviour is approximately close to those in figure 3.6. We will see in the next section that figure 3.11 has important consequences to the pure CDT eigenvalue distribution and its effective potential.

3.4 Continuum limit of CDT

The main idea here follows the procedure of section 3.2. However, now we have the following renormalization for the bare cosmological constants:

$$\mu' = \frac{\mu'_c}{a^2} + \mu \ , \ \mu'^{in} = \frac{\mu'^{in}_c}{a^2} + \mu^{in} \ , \ \mu'^{out} = \frac{\mu'^{out}_c}{a^2} + \mu^{out} \, . \tag{3.41}$$

We shall introduce the critical values:

$$g_c = e^{-\mu'_c} \quad , \quad x_c = e^{-\mu'^{in}_c} \quad , \quad y_c = e^{-\mu'^{out}_c} \quad . \tag{3.42}$$

Note that the joint convergence of (3.35) requires the critical values to be $g_c = 1/2$ and $x_c = y_c = 1$ (See how to find g_c using other methods in section 4.3). The above formula allows us to write,

$$g = g_c\, e^{-a^2\mu} \quad , \quad x = x_c\, e^{-aX} \quad , \quad y = y_c\, e^{-aY} \quad . \tag{3.43}$$

Now if we apply the scaling unto (3.35), we obtain:

$$G_\mu(X, Y, T) = -\log(1 - Z_\mu) \quad ,$$

$$Z_\mu = \frac{\mu}{sinh^2(\sqrt{\mu}T)\left[X + \sqrt{\mu}\, coth(\sqrt{\mu}T)\right]\left[Y + \sqrt{\mu}\, coth(\sqrt{\mu}T)\right]} \, . \tag{3.44}$$

Performing the Laplace's transform of the above equation, we find the finite time propagator of CDT [39]:

$$G_\mu(L_1, L_2, T) = \sqrt{\frac{\mu L_1}{L_2}}\, I_1\left(\frac{2\sqrt{\mu L_1 L_2}}{sinh(\sqrt{\mu}T)}\right) \frac{e^{-\sqrt{\mu}\, coth\left((L_1+L_2)\sqrt{\mu}T\right)}}{sinh\sqrt{\mu}T} \, , \tag{3.45}$$

Here $T \sim at$ and $I_1(x)$ the modified Bessel function of the first kind (see appendices of [39, 40]). To find the disc function, one needs to compute (slightly different for DT):

$$W(\mu, L) = \int_0^{+\infty} dT\, G_\mu(L_1 = L, L_2 = 0, T) \quad . \tag{3.46}$$

Once the integral is calculated, we acquire:

$$W(\mu, L) = \frac{1}{L}\, e^{-\sqrt{\mu}L} \quad , \tag{3.47}$$

Which is the Hartle-Hawking wavefunction of CDT, the analogue of (3.31).

4
Random matrices techniques applied to DT and CDT

In this chapter we introduce two methods for computing matrix integrals: saddle point and orthogonal polynomials. The outline of these methods have enormous importance for further calculations in two dimensional quantum gravity. We use the analogy of a Coulomb gas to construct the saddle point analysis, implementing the resolvent and through it we find how to compute the eigenvalue distribution, where complex analysis play an important role. Afterwards we define a set of orthogonal (or orthonormal) polynomials that remarkably solve the matrix model through a recursion formula. Following the background of these methods, we discuss its application to DT and CDT matrix models, followed by the study of the double scaling limit.

4.1
Saddle point analysis

We want to solve (2.1), but we have seen how to rewrite it to an integral of eigenvalues (2.8). Due to the fact that the potential has one deepest well, the eigenvalues tend to be restricted to the basement of the well. In the Gaussian case the eigenvalue distribution has only one continuous support, i.e the density vanishes outside an interval $\mathcal{I}$ (then called one-cut solution, otherwise it is called a multi-cut solution). In order to better understand the behaviour of $\rho(\lambda)$ regarding the Vandermonde's interaction, we shall include a parameter t (known as 't Hooft parameter) unto (2.8):

$$Z = const \times \prod_i \int d\lambda_i \, e^{-\frac{N}{t}\sum V(\lambda_i)} \Delta^2(\lambda) \quad , \tag{4.1}$$

Thus, we have then an effective potential,

$$V_{eff} = \sum_i V(\lambda_i) - \frac{2t}{N} \sum_{i<j} \ln|\lambda_j - \lambda_i| \quad . \tag{4.2}$$

The saddle point of the action is straightforwardly found:

$$\frac{\partial S}{\partial \lambda_j} \equiv 0 = V'(\lambda_j) - \frac{2t}{N} \sum_{i<j} \frac{1}{\lambda_j - \lambda_i} \quad . \tag{4.3}$$

With such configuration, the factor t manages the strength of the repulsion between the eigenvalues. For small t the eigenvalues tend to be around the the saddle point (when $V'(\lambda_i) = 0$). If t vanishes, the the interval of the eigenvalues collapses to the saddle point. If t increases, the eigenvalues are compelled to disperse over a support of interval $\mathcal{I}$. If one multiplies both sides in (4.2) by $\frac{1}{N}(z-\lambda_j)^{-1}$ and sum over j, it is obtained:

$$\frac{1}{N}\sum_{j=1}^{N}\frac{V'(\lambda_j)}{z-\lambda_j} = \frac{2t}{N^2}\sum_{1\leq i\neq j\leq N}\frac{1}{(z-\lambda_j)}\frac{1}{(\lambda_j-\lambda_i)} \quad . \tag{4.4}$$

Simple algebra can change the form of r.h.s of (4.4), as follows:

$$\frac{1}{N}\sum_{j=1}^{N}\frac{V'(\lambda_j)}{z-\lambda_j} = \frac{t}{N^2}\sum_{i\neq j}\sum_{j}\frac{1}{(z-\lambda_j)}\frac{1}{(\lambda_j-\lambda_i)}+$$

$$\frac{t}{N^2}\sum_{j\neq i}\sum_{i}\frac{1}{z-\lambda_i}\Big(-\frac{1}{\lambda_j-\lambda_i}\Big) \quad ,$$

$$\frac{t}{N^2}\sum_{1\leq i\neq j\leq N}\frac{1}{\lambda_j-\lambda_i}\Big(\frac{1}{z-\lambda_j}-\frac{1}{z-\lambda_i}\Big) = \frac{V'(z)}{N}\sum_{j=1}^{N}\frac{1}{z-\lambda_j}-$$

$$\frac{1}{N}\sum_{j=1}^{N}\frac{V'(z)-V'(\lambda_j)}{z-\lambda_j} \quad .$$

We introduce new quantities. First the resolvent,

$$\omega(z) = \frac{1}{N}\Big\langle \mathrm{tr}\frac{1}{z-M}\Big\rangle \sim \omega_N(z) + \mathcal{O}(\frac{1}{N}) \quad ,$$

$$\omega_N(z) = \frac{1}{N}\sum_{j=1}^{N}\frac{1}{z-\lambda_j} \quad , \tag{4.5}$$

along with a polynomial of two orders below $V'(z)$, defined through

$$P(z) \equiv \lim_{N\to+\infty}\frac{t}{N}\sum_{j=1}^{N}\frac{V'(z)-V'(\lambda_j)}{z-\lambda_j} \quad . \tag{4.6}$$

Accordingly, we rewrite (4.3),

$$V'(z)\omega_N(z) - \frac{1}{t}P_N(z) = \frac{t}{N^2}\sum_{1\leq i\neq j\leq N}\frac{1}{(z-\lambda_j)(z-\lambda_i)} \quad . \tag{4.7}$$

Nevertheless, in the large-N limit we acquire:

$$\omega^2(z) - \frac{1}{t}V'(z)\omega(z) + \frac{1}{t^2}P(z) = 0 \quad , \tag{4.8}$$

Whose solution is (see section 3.1):

$$\omega(z) = \frac{1}{2t}\left[V'(z) - \sqrt{\big(V'(z)\big)^2 - 4P(z)}\right] \quad . \tag{4.9}$$

The eigenvalue distribution reads (because we are evaluating it at the saddle point):

$$\rho(\lambda) = \frac{1}{N}\sum_i \delta(\lambda - \lambda_i) = \frac{1}{N}\sum_i \langle\delta(\lambda - \lambda_i)\rangle \quad , \tag{4.10}$$

And in the planar limit (large-N limit) is normalized as follows

$$\int_{\mathcal{I}} d\lambda\, \rho(\lambda) = 1 \quad . \tag{4.11}$$

Is quite easy to find the eigenvalue density once we have the resolvent. Foremost, let's remind the reader of the Cauchy's formula:

$$f^{(n)}(a) = \frac{n!}{2\pi i}\oint_{\mathcal{I}} dz\, \frac{f(z)}{(z-a)^{n+1}} \quad , \tag{4.12}$$

for the n-th derivative of the function f evaluated at a. As a result,

$$\rho(z) = \frac{1}{2\pi i}\oint_{\mathcal{I}} dz\, \frac{\rho(\lambda)}{\lambda - z} \quad . \tag{4.13}$$

(4.3) together with (4.11) enables us to write,

$$V'(\lambda_j) = \frac{2t}{N}\sum_{i<j} \frac{1}{\lambda_j - \lambda}\delta(\lambda - \lambda_i) \quad . \tag{4.14}$$

Following the same train of thought, we see that

$$\omega(z) = \int d\lambda\, \frac{\rho(\lambda)}{z - \lambda} \quad . \tag{4.15}$$

From (4.13) and (4.15) one obtains,

$$\begin{aligned} \rho(z) &= \lim_{\epsilon\to 0}\int_{z-i\epsilon}^{z+i\epsilon} \frac{d\lambda}{2\pi i}\frac{\rho(\lambda)}{\lambda - z}\,, \\ &= \frac{1}{2\pi i}\lim_{\epsilon\to 0}\Big[\omega(z - i\epsilon) - \omega(z + i\epsilon)\Big]\,. \end{aligned} \tag{4.16}$$

Recalling the expression for the resolvent in (3.19), we can find a general expression for $\rho(z)$ based on the discontinuity equation above. It follows:

$$4\pi i t\rho(z) = \lim_{\epsilon\to 0}\left\{\Big[V'(z-i\epsilon) - V'(z+\epsilon)\Big] + \Big[(gz-c) + i\epsilon\Big]\sqrt{(z + i\epsilon - c_+)(z + i\epsilon - c_-)}\,,\right.$$

$$\left. -\Big[(gz - c) - i\epsilon\Big]\sqrt{(z - i\epsilon - c_+)(z - i\epsilon - c_-)}\right\}. \tag{4.17}$$

Moreover, the discontinuity part of the potential reads:

$$V'(z - i\epsilon) - V'(z + i\epsilon) \sim -const \times 2\epsilon i + \mathcal{O}(\epsilon^2)\,, \tag{4.18}$$

By this means obtaining,

$$\begin{aligned}\rho(z) &= \frac{1}{2\pi t}(gz-c)\sqrt{-(z-c_+)(z-c_-)} \\ &= \frac{1}{2\pi t}\sqrt{4P(z)-\left(V'(z)\right)^2} \quad . \end{aligned} \tag{4.19}$$

Once one knows how to compute the eigenvalue distribution, it is simple to find averages. For instance,

$$\frac{1}{N}\langle \mathrm{tr} M^p\rangle = \int_{\mathcal{I}} d\lambda \rho(\lambda)\lambda^p \quad . \tag{4.20}$$

Even though we have a formula for $\omega(z)$, there is a more powerful technique to express it. Recall the Laurent series:

$$f(z) = a_0 + a_1(z-a) + a_{-1}(z-a)^{-1} + \cdots \quad ,$$

$$a_n = \frac{1}{2\pi i}\oint dz\, \frac{f(z)}{(z-a)^{n+1}} \quad . \tag{4.21}$$

If one wants to compute the residue of $f(z)$ at a for a pole of order k, we would have

$$a_{-1} = \lim_{z\to a}\frac{1}{(k-1)!}\frac{d^{k-1}}{dz^{k-1}}\left[f(z)(z-a)^k\right] \quad . \tag{4.22}$$

Then, we simply expand (4.9) as a Laurent series. For the sake of simplicity, we define a polynomial such that,

$$\mathcal{P}(z) = \frac{V'(z)}{\sqrt{(z-c_+)(z-c_-)}} = (gz-c) + \mathcal{P}_- = \mathcal{P}_+ + \mathcal{P}_- \quad , \tag{4.23}$$

Hence,

$$\omega(z) = \frac{\mathcal{P}_-(z)}{2}\sqrt{(z-c_+)(z-c_-)} = \sum_i \frac{\mathcal{P}_{-i}}{2}\frac{\sqrt{(z-c_+)(z-c_-)}}{z^i} \quad . \tag{4.24}$$

Of course this formulation of the resolvent must obey the large z behaviour of $\omega(z) \sim 1/z$. On the other hand,

$$\begin{aligned}\frac{1}{z} = \lim_{z\to+\infty}\Bigg[&\frac{\mathcal{P}_{-1}}{2}\frac{\sqrt{(z-c_+)(z-c_-)}}{z} + \\ &\frac{\mathcal{P}_{-2}}{2}\frac{\sqrt{(z-c_+)(z-c_-)}}{z^2} + \cdots\Bigg],\end{aligned} \tag{4.25}$$

Which requires:

$$\mathcal{P}_{-2} = 2 \quad ; \quad \mathcal{P}_{-1} = \mathcal{P}_{-k} = 0 \quad \forall\, k\in\mathbb{N}\,,\, k>2 \quad . \tag{4.26}$$

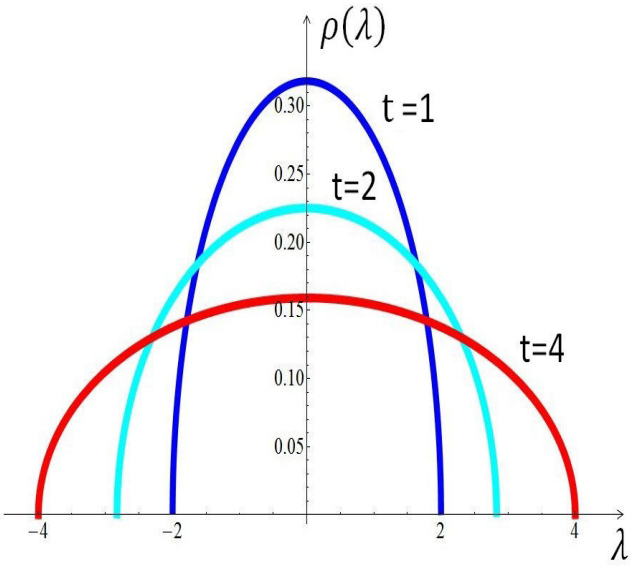

Figure 4.1: Eigenvalue distribution of a Gaussian potential. We show distributions with three different fixed values of t.

From (4.21),(4.23) and (4.26) we find two equations powerful to find out an explicit form of $w(z)$:

$$\oint \frac{dz}{2\pi i} \frac{V'(z)}{\sqrt{(z-c_+)(z-c_-)}} = 0 \quad ,$$

$$\oint \frac{dz}{2\pi i} \frac{zV'(z)}{\sqrt{(z-c_+)(z-c_-)}} = 2t \quad . \tag{4.27}$$

Alternatively, after the following change of variable,

$$z = w + \frac{1}{2}(c_+ + c_-) + \frac{(c_+ - c_-)^2}{16w} \tag{4.28}$$

One obtains instead:

$$\oint \frac{dw}{2\pi i} \frac{V'(z(w))}{w} = 0 \quad ,$$

$$\oint \frac{dw}{2\pi i} V'(z(w)) = t \quad . \tag{4.29}$$

A simple example is given: For a Gaussian potential $V'(\lambda) = \lambda$ (in the above equations we have set $z = \lambda$, not affecting at all its structure. Recall that due to the symmetry of the potential $c_+ = -c_-$ and we have the pole at $w = 0$), so:

$$\lambda = w + \frac{c_\pm^2}{4w} \quad ,$$

Applying (4.22) we arrive at,

$$t = \lim_{w\to 0} \frac{1}{0!} \left[f(w)(w-0)\right] = \lim_{w\to 0} \left[w^2 + \frac{c_\pm^2}{4}\right] \quad \therefore \quad c_\pm = \pm 2\sqrt{t} \quad ,$$

And substituting it unto (4.9) and (4.19), we find:

$$\rho(\lambda) = \frac{\sqrt{4t - \lambda^2}}{2\pi t} \quad . \tag{4.30}$$

Notice that this would have been exactly the expression for the resolvent in (3.17) if we had set $t = 1$. The saddle point gives the large-N limit contribution of the matrix integrals and is not valid for multi-matrix integrals.

4.2 Orthogonal polynomials

Another method to solve the matrix models are the orthogonal polynomials. It can give us the contributions of all orders in the $1/N$ expansion. Yet, it presents a more elegant and easier way to understand the large-N limit. Like saddle point analysis, it can not be applied to multi-matrix models in its simplest formalism. However, its analytic strength allows the extension to general orthogonal polynomials and operators which are able to handle multi-matrix models and fancy mathematical structures [50, 73, 74]. Once again we start with the partition function:

$$Z = \frac{1}{N!(2\pi)} \int \prod_i \frac{d\lambda_i}{(2\pi)} \Delta^2(\lambda)\, e^{-\frac{N}{t}V(\lambda)} \quad . \tag{4.31}$$

Foremost, we introduce a set of orthogonal polynomials which will be useful to compute the partition function. These polynomials have the form,

$$P_n(\lambda) = \lambda^n + \mathcal{O}(\lambda^{n-1}) \quad , \tag{4.32}$$

So that the normalization comes out naturally:

$$\int \prod_i \frac{d\lambda_i}{2\pi} e^{-\frac{N}{t}V(\lambda)} P_\alpha(\lambda) P_\beta(\lambda) = \int d\mu P_\alpha(\lambda) P_\beta(\lambda) = \delta_{\alpha\beta} h_\alpha. \tag{4.33}$$

Is easy to see that $\lambda P_\alpha \sim \lambda^{\alpha+1} + \mathcal{O}(\lambda^\alpha) \sim P_{\alpha+1}$, implying:

$$\int d\mu (\lambda P_\alpha) P_{\alpha+1} = h_{\alpha+1} \quad \text{or} \quad \int d\mu P_{\alpha+2} (\lambda P_{\alpha+1}) = h_{\alpha+2} \quad . \tag{4.34}$$

The form of these polynomials enable us to express them as a linear combination of one to another, as follows:

$$\lambda P_\alpha = \sum_{k=0}^{\alpha+1} \sigma_\alpha^k P_k \quad , \quad \sigma_\alpha^k = \frac{1}{h_k} \int d\mu \lambda P_\alpha P_k \neq 0 \Leftrightarrow |\alpha - k| = 1\,. \tag{4.35}$$

Accordingly,

$$\lambda P_\alpha = P_{\alpha+1} + \left(\frac{h_\alpha}{h_{\alpha-1}}\right) P_{\alpha-1} = P_{\alpha+1} + r_\alpha P_{n-1} \quad . \tag{4.36}$$

The above recursion relation can be generalized and it is a special case for even potentials. The most general relation is:

$$\lambda P_n(\lambda) = P_{n+1}(\lambda) + s_n P_n(\lambda) + r_n P_{n-1}(\lambda) \quad . \tag{4.37}$$

The reason is plain. Let us reconsider (4.28) and (4.29): It can be written as (in the planar limit)

$$X(r,s) \equiv \oint \frac{dw}{2\pi i} \frac{V'(w + s + \frac{r}{w})}{w} = 0 \quad ,$$

$$Y(r,s) \equiv \oint \frac{dw}{2\pi i} V'(w + s + \frac{r}{w}) = t \quad . \tag{4.38}$$

Roughly speaking, for even potentials the support of the eigenvalue density is the interval $[-a, a]$, then we conclude that s automatically vanishes. An important feature of the recursion relations is that it is an hermitian operation. In other words, does not matter which of the two polynomials, $P_\alpha(\lambda)$ or $P_\beta(\lambda)$, is multiplied by λ. For instance,

$$\langle P_{n+1}|\lambda P_n\rangle = \int d\mu\, P_{n+1}(\lambda P_n) = \int d\mu\, P_{n+1}(P_{n+1} + s_n P_n + r_n P_{n-1}) = h_{n+1} \quad ,$$

On the other hand,

$$\langle \lambda P_{n+1}|P_n\rangle = \int d\mu\, P_n(\lambda P_{n+1}) = \int d\mu\, P_n(P_{n+2} + s_{n+1} P_{n+1} + r_{n+1} P_n) = r_{n+1} h_n \quad ,$$

which is exactly the same of the latter. Therefore,

$$\int d\mu\, \lambda\, P_\alpha P_\beta = \langle \lambda P_\alpha | P_\beta\rangle = \langle P_\alpha | \lambda P_\beta\rangle \quad . \tag{4.39}$$

Now that we have a general recursion relation, we urge to figure out how to associate the square of Vandermonde's determinant with the polynomials mentioned. See appendix C.1 for such a procedure. In fact, the partition function can be written as a function of the normalization of the polynomials, namely:

$$Z = \prod_{i=1}^{N-1} h_i = h_0^N \prod_{i=1}^{N} r_i^{N-i} \quad . \tag{4.40}$$

Naturally, the next step is to find a nice expression for the free energy. We acquire:

$$F = N \ln h_0 + \sum_{i=1}^{N} (N-i) \ln r_i \quad . \tag{4.41}$$

Recall the topological expansion of the matrix integral's free energy (2.27). We now take into account the 't Hooft parameter t. We shall rewrite it as,

$$F(t) = \sum_{h=0}^{+\infty} g_s^{2h-2} F_h(t) \quad , \quad t = g_s N \quad . \tag{4.42}$$

By virtue of that, we revise (4.41)

$$\frac{1}{N^2} F = \frac{1}{N} \ln h_0 + \frac{1}{N} \sum_{i=1}^{N} (1 - \frac{i}{N}) \ln r_i \quad . \tag{4.43}$$

Well, in the planar limit the sum becomes an integral. Besides, the ratio i/N turns into a variable, henceforth denoted by ξ. In addition, the first term of the r.h.s of (4.43) vanishes. Hereby,

$$F_0(t) = t^2 \int_0^1 d\xi \, (1 - \xi) \ln r(\xi) = t^2 \int_{r(\xi=0)}^{r(\xi=1)} dr \, \frac{d\xi}{dr} \, (1 - \xi) \ln r(\xi) \quad . \tag{4.44}$$

Nevertheless, we don't know how ξ depends on the planar limit contribution of r_n. The bridge between the recursion relations and the free energy are the string equations. The equations are written as (see appendix C.2)

$$\int d\mu \, P_n(\lambda) \, V'(\lambda) \, P_n(\lambda) = 0 \quad ,$$

$$\int d\mu \, P_{n-1}(\lambda) \, V'(\lambda) \, P_n(\lambda) = \frac{\xi_n h_n}{r_n} t \quad . \tag{4.45}$$

A rather simple way to derive the string equations comes from transforming (4.37) into a matrix recursion relation (actually, the aim of such extension to generalized formulae of the polynomials is far beyond the need for a derivation of the string equations). That is, we define two matrices A and B which obeys the relations ($AP = \partial_\lambda P$ and $BP = \lambda P$ so that $[B, A] = \mathbb{1}$):

$$\partial_\lambda P_n = \sum_{m=0}^{n-1} A_{nm} P_m \quad ; \quad \lambda P_n = \sum_{m=0}^{n+1} B_{nm} P_m \quad . \tag{4.46}$$

Within this formulation, (4.39) still holds. We revise (4.33):

$$\int d\mu P_m P_n = h_m \delta_{mn} = H_{mn} \quad . \tag{4.47}$$

Hence,

$$\int d\mu \Big(\sum_{i=0}^{n+1} B_{ni} P_i \Big) P_m = (B_{ni} \delta_{mi}) h_m = B_{ni} (\delta_{mi} h_m) = BH \quad ,$$

$$\int d\mu \, P_n \left(\sum_{j=0}^{m+1} B_{mj} P_j \right) = (h_n \delta_{nj}) B_{mj} = h_n (\delta_{nj} B_{mj}) = H B^T \, . \tag{4.48}$$

Therefore,

$$HB^T = BH \quad . \tag{4.49}$$

If we follow the derivation of the string equations, specially the vanishing integral (C.11), we would have

$$\frac{N}{g}V'_{nm}s_m = \int d\mu\, P'_n P_m + \int d\mu\, P_n P'_m \quad , \tag{4.50}$$

Where $V'_{nm} = V'(\lambda)\delta_{nm}$. Additionally, we have:

$$\begin{aligned} \int d\mu \left(\sum_{k=0}^{n-1} A_{nk}P_k\right) P_m &= A_{nk}(\delta_{km}h_m) = (A_{nk}\delta_{km})h_m = AH \quad , \\ \int d\mu\, P_n \left(\sum_{l=0}^{m-1} A_{ml}P_l\right) &= (h_n\delta_{nl})A_{ml} = h_n(\delta_{nl}A_{ml}) = HA^T \quad . \end{aligned} \tag{4.51}$$

Leading to,

$$AS + SA^T = \frac{N}{g}V'(B)S \quad . \tag{4.52}$$

Doing the normalization (4.47), It is straightforward to see:

$$A_{n,n-1} = n \quad ; \quad B_{n-1,n} = B_{n,n+1} = 1 \quad . \tag{4.53}$$

Is easy to check from (4.52) and (4.53) that if $m = n-1$ is set, we attain the string equations in the matrix version:

$$V'_{n,n} = 0 \quad ; \quad V'_{n,n-1} = \xi_n t \quad . \tag{4.54}$$

Alternatively, one might want to work with orthonormal polynomials. They are chosen to obey

$$\int d\mu\, \Pi_n \Pi_m = \delta_{mn} \quad , \quad \Pi_n(\lambda) = \frac{1}{\sqrt{s_n}} P_n(\lambda) \quad . \tag{4.55}$$

We immediately arrive at:

$$\lambda\Pi_n = \sqrt{r_{n+1}}\,\Pi_{n+1} + s_n\,\Pi_n + \sqrt{r_n}\,\Pi_{n-1} \quad . \tag{4.56}$$

This is useful for computing averages. For example we can compute (4.20):

$$\left\langle \mathrm{tr}M^l \right\rangle = \frac{1}{N!Z}\int d\mu \Delta^2(\lambda) \left(\sum_i \lambda_i^l\right) \quad . \tag{4.57}$$

Useful formulae from (4.40), (C.2) and (C.3) enable us to go further:

$$\begin{aligned} \left\langle \mathrm{tr}M^l \right\rangle &= \frac{1}{N!\prod_i h_i} \sum_i \int d\mu \left(N! \prod_i h_i \Pi_i^2\right) \lambda_i^l \\ &= \sum_{i=0}^{N-1} \int d\mu\, \lambda^l \Pi_i^2(\lambda)\,. \end{aligned} \tag{4.58}$$

4.3 Eigenvalue distributions and critical points

We shall discuss the critical points of eigenvalue distributions for higher order potentials. In figure 4.1 is depicted the distribution of the Gaussian case, notice that the repulsion increases along with the values of t. Interesting though, is that for $t = 0$ the repulsion is gone (see (4.2)) and we have a singularity (figure C.4), because the saddle point of the Gaussian potential is found at $\lambda = 0$. Now we need to compute the distributions for higher order potentials. Following matrix arguments based on (4.20) and (4.58) (see [81, 61]), one finds an expression to compute the eigenvalue distribution:

$$\rho(\lambda) = \frac{1}{\pi}\int_0^1 \frac{d\xi}{\sqrt{4r(\xi) - [\lambda + s(\xi)]^2}}\,\theta(4r(\xi) - [\lambda + s(\xi)]^2) \quad , \tag{4.59}$$

θ being the Heaviside's step function. As an example we can compute once again the eigenvalue distribution for the Gaussian potential. Firstly, we are obligated to find $r(\xi)$ and $s(\xi)$. In order to do so, we better apply the string equations. The eigenvalue distribution of the Gaussian potential is computed by (See appendix C.3),

$$\rho(\lambda) = \frac{1}{\pi}\int_0^1 \frac{d\xi}{\sqrt{4t\xi - \lambda^2}}\,\theta(4t\xi - \lambda^2) \quad .$$

However, after a change of variables ($y = 4t\xi - \lambda^2$) and integration by parts we acquire:

$$\begin{aligned}\rho(\lambda) = \frac{1}{4\pi t}\int_{-\lambda^2}^{4t-\lambda^2} \frac{dy}{\sqrt{y}}\,\theta(y) &= \frac{1}{4\pi t}\left[2\sqrt{y}\theta(y) - 2\int dy\delta(y)\sqrt{y}\right]_{-\lambda^2}^{4t-\lambda^2} \quad , \\ &= \frac{1}{2\pi t}\sqrt{4t - \lambda^2} \quad , \end{aligned} \tag{4.60}$$

Matching exactly the previous result (4.30). We already know the function r, after plugging it unto (4.45) one easily finds the free energy. In appendix C.3 we show how to compute the free energy for some cases. Another way to find the resolvent apart from (4.27) or (4.29) is found from a discontinuity equation which can be derived using (4.14) and (4.15)(see also [50]). It reads:

$$\omega(z) = \frac{\sqrt{(z - c_+)(z - c_-)}}{2\pi i t}\int_{c_-}^{c_+} \frac{V'(\lambda)d\lambda}{(\lambda - z)\sqrt{(\lambda - c_+)(\lambda - c_-)}} \quad . \tag{4.61}$$

To find what exactly a is we can use either (4.29) or (4.59). Notice in the example of the Gaussian potential in (4.62) that there is an easier way to find the support $[c_-, c_+]$: the zeros of the denominator. Thereupon, it is

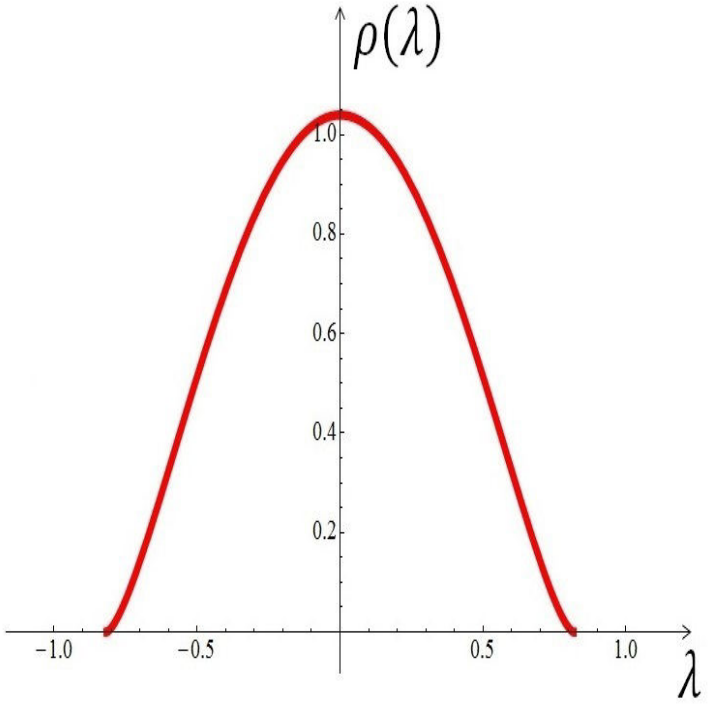

Figure 4.2: Eigenvalue distribution for a quartic potential when $t = t_c$ and $g = 1$.

straightforward to see the following:

$$c_{\pm}(t) = \pm 2\sqrt{r(\xi = 1)} - s(\xi = 1) \quad . \tag{4.62}$$

The reason we want to find the resolvent is very simple: is not quite easy to perform (4.59) when $s \neq 0$ and because we can solve (4.61) with (4.62) as an alternative. As a consequence we should plug the found resolvent unto (4.19). One might compute the resolvent of the quartic potential ($c_{\pm} = \pm a$):

$$\begin{aligned} \omega(g, z) &= \frac{\sqrt{z^2 - a^2}}{2\pi i t} \int_{-a}^{+a} \frac{(\lambda - g\lambda^3)\, d\lambda}{(\lambda - z)\sqrt{\lambda^2 - a^2}} \quad , \\ &= \frac{1}{2t}\left[(z - gz^3) - \left(1 - gz^2 - \frac{1}{2}ga^2\right)\sqrt{z^2 - a^2}\right] . \end{aligned} \tag{4.63}$$

Furthermore, using (4.62) and (C.18) we find:

$$a^2 = c_{\pm}^2(g) = \frac{2}{3g}(1 - \sqrt{1 - 12gt}) \quad . \tag{4.64}$$

Hence, the eigenvalue distribution is,

$$\rho(\lambda) = \frac{1}{2\pi t}\left[1 - g\lambda^2 - \frac{1}{3}(1 - \sqrt{1 - 12gt})\right]\sqrt{\frac{2}{3g}(1 - \sqrt{1 - 12gt}) - \lambda^2} \quad . \tag{4.65}$$

In this case we see that the limiting value for the 't Hooft parameter is around 0.08 in figure C.4, which is actually an approximation of the critical point

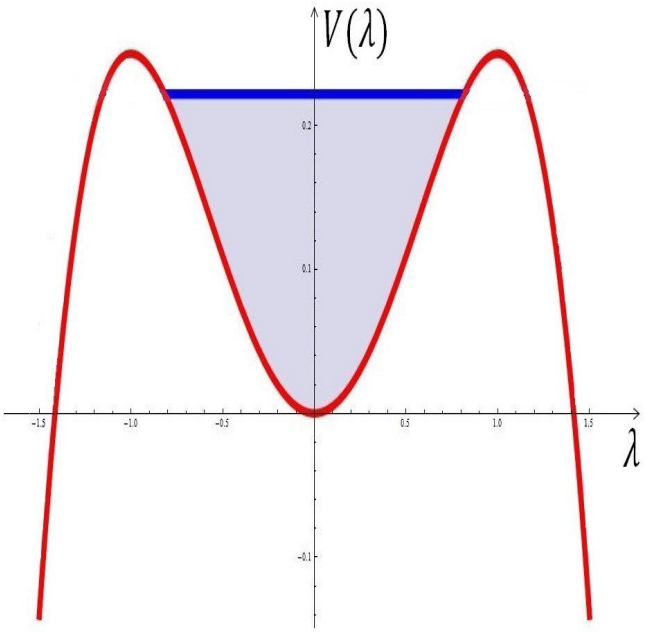

Figure 4.3: Quartic potential with the Fermi level (blue bar) of the potential associated with the outermost eigenvalue when $g = 1$.

$t_c = 1/12$. So, unlike the Gaussian potential, the quartic potential assumes a distribution that does not exists for all t, i.e there is a limit for the strength of the repulsion as seen in figure C.4 (one might be suspicious that all even potentials admit eigenvalue distributions defined for every value of t because of the absence of s in the recursion relation (4.37), expecting funny behaviour from odd potentials only). It is important to realize that although the critical values of t and g coincide for the quartic potential (see another method to achieve g_c in appendix B), this does not happens for the DT and CDT cases. Note also that the critical value can be extracted from the functions $r(1)$: Equation (C.18) allows us to do so. clearly, one should understand that the maximum value of $r(1)$ is $1/6$ when $t = t_c = 1/12$. Recalling that the maximum values for the eigenvalues are formulated in (4.62), the furthermost eigenvalue would be $\sqrt{2/3} \approx \pm 0.816$. Remarkably, this result agrees with figure C.4, where the maximum eigenvalue appears to be about ± 0.8. For better visualization though, we show the same distribution at the critical point $t = t_c$ in figure 4.2, which turns out to be

$$\rho(\lambda) = \frac{(4 - 6\lambda^2)}{\pi}\sqrt{\frac{2}{3} - \lambda^2} \quad . \tag{4.66}$$

The potential evaluated in the maximum eigenvalue is about 0.222, therefore the eigenvalue region corresponds to the region shadowed in figure 4.3 (bounded by the blue bar). This blue bar is identified with the Fermi level (chemical potential), which is the the difference between the highest and lowest excited

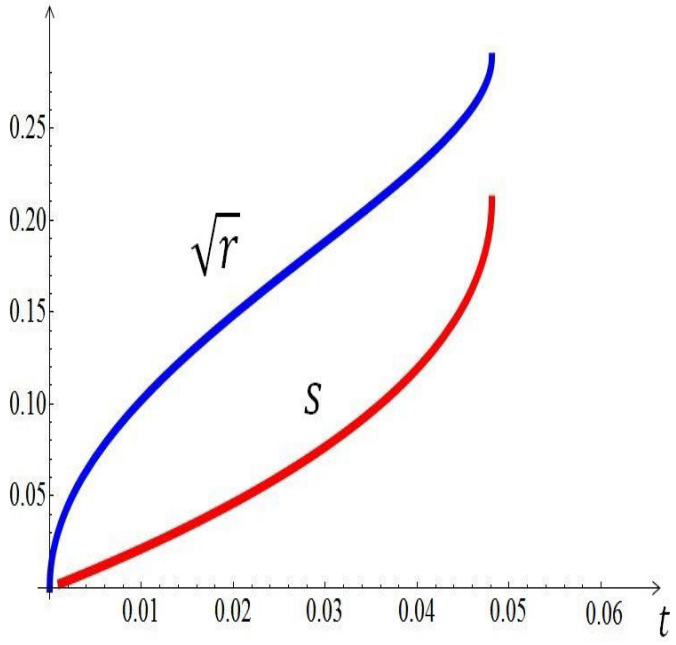

Figure 4.4: behaviour of the functions $\sqrt{r(1,t)}$ and $s(1,t)$.

states, in what might be thought of a electron gas in a metal. As a remark we observe that the Fermi level shall not be confused with the Fermi energy (defined at zero temperature), since there still are interactions, although the value of t diminishes the strength of the interaction fiercely. We shall now make comparisons between DT and CDT through the resolvent, distributions and the effective potential. The string equations for both matrix models are summarized in (C.22),(C.23) and (C.24). Because the functions $r(\xi)$ are way more complicated in the case of odd potentials, not to mention that $s(\xi)$ does not vanish any longer, these integrals are extremely difficult to handle. We now put (4.61) into practice:

$$\omega_{DT}(g,z) = \frac{\sqrt{(z-c_+)(z-c_-)}}{2i\pi t}\int_{c_-}^{c_+}\frac{(\lambda - g\lambda^2)\,d\lambda}{(\lambda - z)\sqrt{(\lambda-c_+)(\lambda-c_-)}} \quad . \tag{4.67}$$

Even for a mathematical software it would take much time to evaluate this integral when $s \neq 0$. Its faster to compute the integral with a denominator like $\sqrt{\lambda^2 - a^2}$. Therefore, we need a change of variables. We choose the new variable to be $y = \lambda + s(1)$ and the radius $a^2 = 4r(1)$, obtaining:

$$\omega(z) = \frac{\sqrt{(z+s(1))^2 - a^2}}{2i\pi t}\int_{-a}^{a}\frac{V'(y)\,dy}{(y - z - s(1))\sqrt{y^2-a^2}} \quad . \tag{4.68}$$

It follows (see appendix C.3):

$$\omega_{DT}(g,z) = \frac{1}{2t}\left\{z - gz^2 - \left[1 + gs_e(1) - gz\right]\sqrt{(z+s_e(1))^2 - a_e^2}\right\} \quad , \tag{4.69}$$

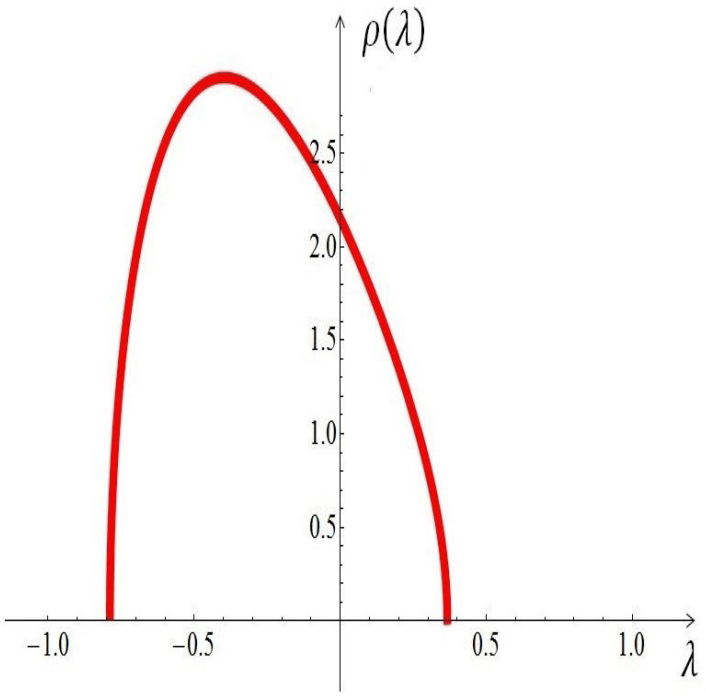

Figure 4.5: Eigenvalue distribution of the DT matrix model at the critical point $t = t_c$ and $g = 1$.

$$\rho_{DT}(\lambda) = \frac{1}{2\pi t}\left[1 + g s_e(1) - g\lambda\right]\sqrt{a_e^2 - (\lambda + s_e(1))^2}\Big] \quad , \tag{4.70}$$

Here we associate DT quantities with the label e (which stands for Euclidean) whilst l (Lorentzian) for CDT. The derivative of the CDT potential adds a term $-g$ to the DT counterpart. For a linear potential the integral in (4.73) is equivalent to

$$\int_{-a}^{a} \frac{dy}{(y - z - s(1))\sqrt{y^2 - a^2}} = \frac{i\pi}{\sqrt{(z + s(1))^2 - a^2}} \quad . \tag{4.71}$$

Thusly, we note that (4.69) is changed by a factor $(-g/2t)$ only (of course the values of s and a^2 are different). Likewise, We would expect that (4.70) does not change its 'structure' (by structure we mean the formula not considering the explicit forms of s and a^2). Even if we did not compute (4.71), it is quite clear why we don't have any change in the structure of the CDT eigenvalue distribution. In the case we have a potential $V(\lambda) = -g\lambda$ the string equations would give $r = s = 0$. Applying it to (4.59) we clearly understand that $\rho(\lambda) = 0$, i.e the $-g$ contribution to the 'structure' of the eigenvalue distribution is null, although the $-g$ does affect the functions $r(\xi)$ and $s(\xi)$ dramatically. Therefore,

$$\omega_{CDT}(g, z) = \frac{1}{2t}\left\{-g + z - gz^2 - \left[1 + g s_l(1) - gz\right]\sqrt{(z + s_l(1))^2 - a_l^2}\right\} \quad , \tag{4.72}$$

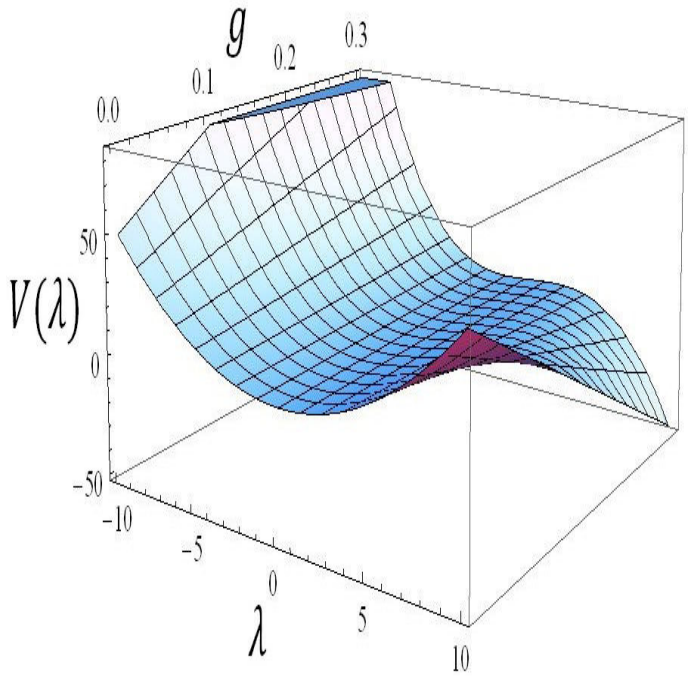

Figure 4.6: DT potential for different values of g. Note that when g is near zero the potential is symmetric relative to the vertical axis (Gaussian potential limit). However, when g increases the potential slowly becomes more asymmetric, whereas the saddle point is at the left side ($\lambda < 0$).

$$\rho_{CDT}(\lambda) = \frac{1}{2\pi t}\left[1 + g s_l(1) - g\lambda\right]\sqrt{a_l^2 - (\lambda + s_l(1))^2}\Big] \quad . \tag{4.73}$$

The distributions are illustrated with the choice $g = 1$, only to make fair comparison with the Wigner's semicircle law. We shall use the functions r and s to find the farthermost eigenvalue. The attainment of the maximum values of either r and s consists of a simple task, once noticing that the critical value of t for both functions is exactly $1/\sqrt{432} \approx 0.048$, and then applying it back to the functions. Remark: In chapter three is pointed out the critical value of g and how it is obtained. From (C.38) and (C.39) one understands that we can find critical values for both g and t. The role of these two parameters are distinct and in the literature it is often interchangeable. For instance, [81] uses t for the 't Hooft parameter and g for coupling whilst [50, 51] associates the g for both purposes. As an example, in DT (see chapter 3) the critical value of the coupling g is $1/\sqrt[4]{432}$ and another way to extract it apart from (D.7) or the radius of convergence of $w_1(g)$) is to consider the limiting values r and s for fixed t. Figure 4.6 shows these functions for a fixed $g = 1$, one can easily obtain the maximum value of t studying the form of α_1 in (C.38). Analogously if we fix $t = 1$ we achieve the critical value of g again from (C.38). As discussed previously, the coupling g does not take part of the role of t, which is to rule the intensity of the interaction. Figure 4.4 exhibits these functions, which shows

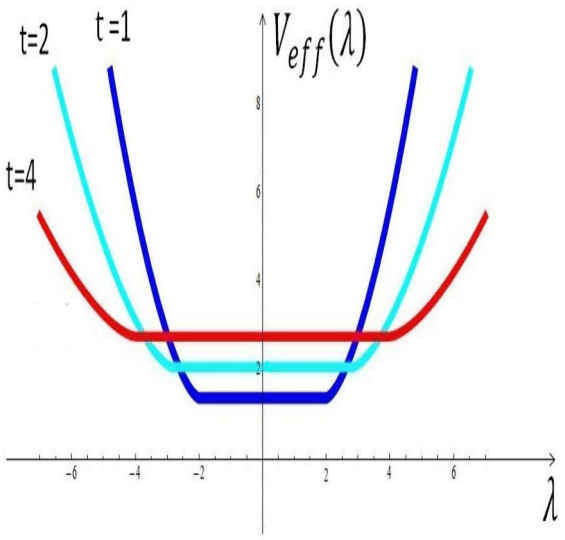

Figure 4.7: Effective potential of the Gaussian case.

a halt around $t = 0.05$, agreeing with the value of t_c. It follows then that the maximum value for an eigenvalue is

$$\lambda_{\pm} = \pm\frac{\sqrt{3}}{3} - \frac{(3-\sqrt{3})}{6} \approx 0.366 \quad \text{or} \quad -0.788 \quad ,$$

Which is corroborated by figure 4.5. Observe that for general odd potentials the eigenvalue distribution is not symmetric relative to the vertical axis, unless the distribution vanishes. This is due the fact that s does not vanishes. The reason for the the eigenvalue distribution be more to the left is due to the position of the saddle point, which in this case is negative (figure 4.6). Additionally, the DT fermi level of the DT potential is lower than for the quartic potential because t_c also has decreased. Without surprise, the eigenvalue function does not exists everywhere in CDT either, and it is not symmetric. The matrix model expression for the CDT partition function is [39, 72]:

$$Z_{CDT} = Z_{\beta}(g, N) = \int d\lambda \, exp\Big[-\frac{N}{t\beta}(-g\lambda + \frac{1}{2}\lambda^2 - \frac{g}{3}\lambda^3)\Big] \quad , \qquad (4.74)$$

As pointed out before (section 3.2) the factor β has the same role of t in the special case of Lorentzian dynamical triangulations, regardless whether it is defined inside or outside the potential. Peculiarly, we know from (3.36) that the CDT matrix model does not evanesce if β vanishes (this β is not the Dyson's index, rather the topology change coefficient in the CDT loop equation), rather it becomes the pure CDT model, i.e quantum gravity without topology change. Figure 3.11 reveals the character of the complex support $[c_-, c_+]$ in the regime of pure CDT: It vanishes. Now, if the support no longer

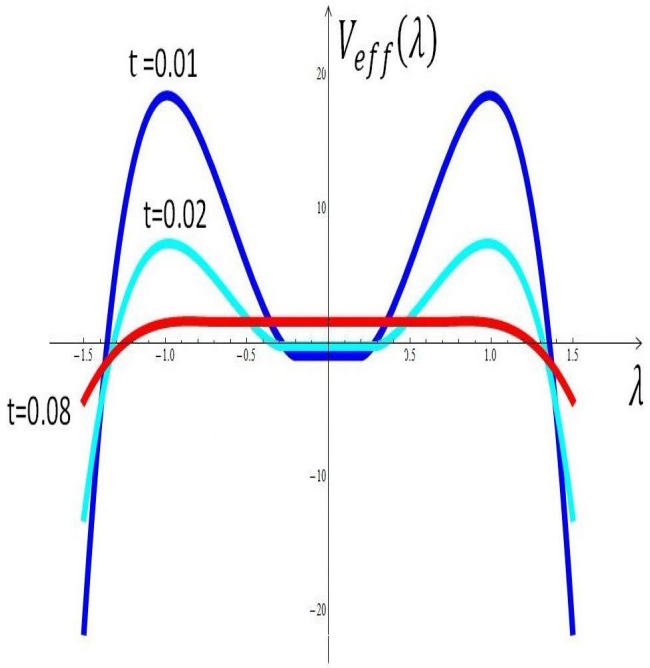

Figure 4.8: Effective potential of the quartic case when $g = 1$.

exists, we have as a direct consequence the disruption of the repulsion between the eigenvalues. Therefore, the distribution of pure CDT is a singularity at the origin. This can be thought of a Fermi gas at zero temperature. In the Dyson gas analogy, whenever t goes to zero we have a scenario where the temperature vanishes. Analogously, in the pure CDT regime of β approaching zero also implies the same phenomena. We have non-interacting fermions occupying different levels up to the Fermi energy (which is exactly the Fermi level in this situation), implying that the mean occupation numbers are, in a very good approximation, step functions. Likewise, the probability of finding the eigenvalue is one at the origin and zero elsewhere. Also interesting is the fact that the pure CDT effective potential is flat, which gives a picture (taking as an example of the figure 4.3) that the Fermi level tends to zero in this case . For a pedagogical calculation of the Fermi energy of the quartic potential see [75]. Further analysis of (C.33) and (C.34) shows that the critical value of t is either 0 or $i/4$ and the critical value of g is equal to $1/2$, which supports the Fermi gas at zero temperature interpretation: if $t_c = 0$ then we would have $\rho(\lambda)$ blowing up around $\lambda = 0$. However, one might not be convinced of the breakdown of the eigenvalue interactions yet. Nonetheless, we still have another powerful tool to confirm this: The plot and explicit form of the effective potential. We can generalize (2.12) in the following way:

$$V_{eff}(\{\lambda_i\}) = \sum_i V(\lambda_i) - \frac{2\Psi t}{N} \sum_{i<j} \ln|\lambda_j - \lambda_i| \quad , \tag{4.75}$$

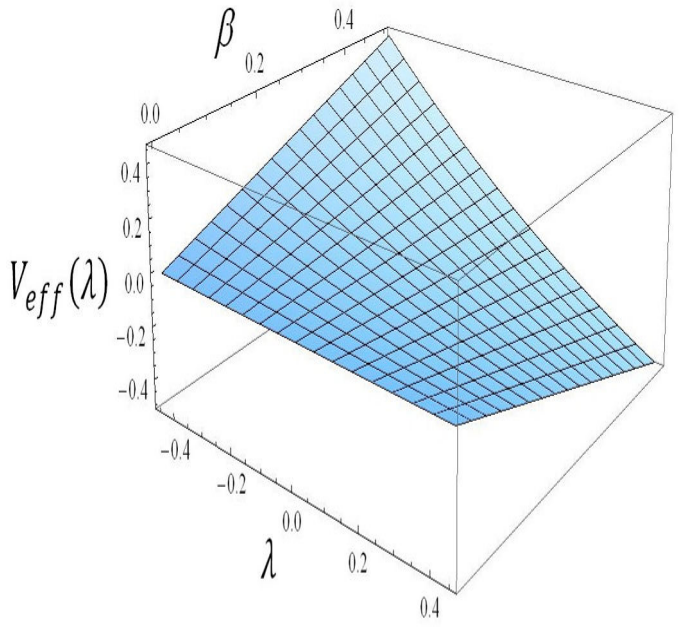

Figure 4.9: Effective potential of CDT when $g = t = 1$.

Where $\Psi = \beta$ for CDT and $\Psi = 1$ otherwise. Of course it is not easy to find a simple expression for the above formula. Instead, we shall use the very good approximation (as $N \to \infty$) for the effective potential of the N-th eigenvalue $\lambda_N \equiv x$ (see [76] and recall (4.74)):

$$V_{eff}(x) \approx -\Psi \mathrm{Re}\left[\int^{x} dz \sqrt{\left(V'(z)\right)^2 - 4P(z)}\right] \quad . \tag{4.76}$$

With this in mind, we can assure the results discussed earlier in this section. Clearly the effective potential is controlled by β either in (4.75) or (4.76). As argued before, we have the following scenario: If β approaches zero there is a disruption of the interaction and the correspondent Fermi level completely vanishes. In figure 4.8 we can see what was explained: When $\beta = 0$ the effective potential becomes a straight line passing through the origin, the effective potential felt by all eigenvalues is zero, there is no repulsion between the eigenvalues whatsoever in pure CDT. Moreover, Figure 4.7 shows the approximate value of the outermost eigenvalue for the quartic potential (the interval of the support is actually the plateau of the effective potential) is about ± 0.9, agreeing with figure 4.2. Also, whenever t approaches its critical value the graphic flattens. In the CDT case this effect would be inverted, since the 'real' critical point is zero, then explaining why the pure CDT potential is flattened and the Fermi level decreases until it vanishes. On the other hand, the effective potential of the Gaussian potential in figure 4.9 shows that there is no critical point in the plot, implying that indeed t has no bound and the higher the value of t the effective potential becomes flatter.

4.4 Double scaling limit

Let's analyse the recursion relations and its consequences towards the continuum limit of the potential $gV'(\lambda) = \lambda + 2\lambda^3 + 3b\lambda^5$ (we have set $t = 1$):

$$g\xi_n = r_n \left\{ 1 + 2\big(r_{n+1} + r_n + r_{n-1}\big) + 3b\Big[r_{n+1}(r_{n+2} + r_{n+1} + r_n) + r_n(r_{n+1} + r_n + r_{n-1}) + r_{n-1}(r_n + r_{n-1} + r_{n-2}) + r_{n+1}r_{n-1} \Big] \right\} \quad , \quad (4.77)$$

Having the approximate behaviour:

$$g\xi \approx W(r) + (2r + 30br^2)\Big[r(\xi + \epsilon) + r(\xi - \epsilon) - 2r \Big] \quad . \quad (4.78)$$

From the basics of Calculus we can simplify the second term of the above equation:

$$\begin{aligned} g\xi &= W(r) + (2r + 30br^2)\epsilon^2 r''(\xi) \quad , \\ &\sim W(r) + \epsilon^2(2r + 30br^2)r''(\xi) \quad . \end{aligned} \quad (4.79)$$

We can go further by making an expansion of $W(r)$ around its critical point, i.e $W'(r_c) = 0$ (first critical region). It reads:

$$W(r) \approx g_c + \frac{1}{2}W''(r_c)(r - r_c)^2 \quad . \quad (4.80)$$

Meanwhile,

$$W''(r_c) = \frac{d^2}{dr^2}\bigg|_{r=r_c} \Big[r + 6r^2 + 30br^3 \Big] = 12(1 + 15br_c) \quad , \quad (4.81)$$

Implying,

$$g\xi = g_c + 6(1 + 15br_c)(r - r_c)^2 + 2\epsilon^2 r_c(1 + 15br_c)r''(\xi) \quad . \quad (4.82)$$

If we set :

$$g_c - g\xi = a^2 g_c x \quad ; \quad r = r_c\big(1 - u(x)\big) \quad , \quad (4.83)$$

It follows right away,

$$\frac{g\xi - g_c}{(6 + 90br_c)} = r_c^2 a^2 u^2 - \frac{1}{3}\epsilon^2 r_c \left(\frac{g}{g_c}\right)^2 a^{-3} r_c u''(x) \quad . \quad (4.84)$$

Hence, identifying $\epsilon = a^{5/2}$ and considering g very near to its critical value, the equation now reads:

$$\alpha x = u^2 - \frac{1}{3}u''(x) \quad , \quad \alpha = -\frac{g_c}{r_c^2(6 + 90br_c)} \, , \quad (4.85)$$

Which is known as Painlevé I equation. Using (4.70) in the planar limit, we obtain:

$$r - r_c \sim (g_c - g\xi)^{1/2}. \tag{4.86}$$

One could generalize this expression to

$$\frac{f}{f_c} - 1 \sim (g_c - g\xi)^{-\gamma} \quad , \quad f = f(\xi) = f(r(\xi)) \quad . \tag{4.87}$$

We shall analyse the behaviour of the free energy in the double scaling limit ($N \to \infty$ at the same time as $g \to g_c$). First we use Taylor's series to make the approximation $\ln(1+\delta) \approx \delta$ (for small δ). Ergo, we can write down the expression of the free energy (4.45) in the double scaling limit :

$$\frac{1}{N^2}F \approx \int_0^1 (1-\xi)\,(g_c - g\xi)^{-\gamma}\, d\xi \approx \frac{g_c^{-\gamma}}{(1-\gamma)(2-\gamma)}\left(1 - \frac{g}{g_c}\right)^{2-\gamma} \quad , \tag{4.88}$$

The last equation can be approximated as,

$$\frac{1}{N^2}F \approx \sum_{n=1}^{+\infty} \frac{1}{g_c^{-\gamma}\Lambda(\gamma)}\, n^{\gamma-3} \left(\frac{g}{g_c}\right)^n \sim \sum_n n^{\gamma-3}\left(\frac{g}{g_c}\right)^n \quad . \tag{4.89}$$

The last approximation is an important result, because it relates the continuum Liouville Theory critical exponents to the ones in the discrete approach (topological expansion). Notice for example that if we choose $\gamma = 3$ we would have $(1 - g/g_c)^{-1} = \sum_n (g/g_c)^n$ instead, which is a very known and trivial expansion. Finally, we shall compute the second derivative of the free energy, which is:

$$\frac{d^2}{d\mathcal{X}^2}\left(\frac{1}{N^2}F\right) = \frac{g_c^{-2}}{(1-\gamma)(2-\gamma)}\mathcal{X}^{-\gamma} \quad , \quad \mathcal{X} \equiv g_c - g = a^2 g_c x(1). \tag{4.90}$$

The Painlevé equations are important because once one applies it to the generalized operator formalism (see [73, 74]) it becomes related to KdV flows [50]. Albeit we did not address the general operator formalism here, it has crucial role in topological gravity [77, 78, 79, 80, 81], Kontsevich matrix model [82] and non-critical string theory in $D = 0$ target space [83, 84, 85]. Finally but not least, equation (4.88) reveals the singular behaviour of the free energy which is essential in the study of multicritical regions (see [50]), that is:

$$Z(g) \sim -\frac{N^2 m^2}{(m+1)(2m+1)}\left(1 - \frac{g}{g_c}\right)^{2+\frac{1}{m}} \quad , \tag{4.91}$$

Where m denotes the *m-th* critical point.

5
Summary and outlook

In this thesis two different techniques to tackle the two-dimensional quantum gravity problem were outlined, using log-gas analogy in matrix models to study the eigenvalue distribution function for an arbitrary potential. Even though the two-dimensional quantum gravity consists of a toy model, it is worth studying due to being analytically solvable either in continuum or discrete approaches. The orthogonal polynomial approach gives us knowledge to find quantities like the free energy in the planar limit (all order corrections as well [72]) and the eigenvalue distribution. We analysed in a fair depth the consequences of using odd potentials in matrix models. Fortunately, matrix models can be applied to a recent discovered non-perturbative approach for the path integral formulation of gravity which in turn is defined through causal dynamical triangulations (which is described by odd potentials). We have shown the difficulty to compute quantities in the DT/CDT scenario, and its stunning conclusions, like the asymmetrical distribution, the existence of a bound of the parameter t and the zero temperature Fermi gas limit when $\beta = 0$ in CDT, in addition we plotted the effective potential for different cases, in particular showing that in the pure CDT we reach the null interaction. Furthermore, we showed how to encounter the Painlevé differential equation in the double scaling limit and by this means obtaining an agreement between continuum and discrete approaches regarding the topological expansion.

A open problem consists in finding a rigorous proof of the equivalence of continuum and discrete approaches, although there is evidence to believe they are perfectly compatible [52, 86]. An important next step would be the study of the continuum matrix model of CDT (see [39]). It would be useful to stud an extension of this work to multi-matrix models, not to mention the inclusion of matter fields. Another further step forward would consist of applying CDT matrix model to study ZZ brane amplitudes through instanton sectors, an extension of the result for DT matrix model in [87].

A
Vandermonde's determinant

In this appendix we show how to integrate out the unitary degrees of freedom in the partition function of a $N \times N$ hermitian matrix ensemble. In the case of the one matrix model the partition function is expressed as in (2.8). Noting the eigenvalue decomposition $M = U^{\dagger}\Lambda U$, we shall change from integrating over all elements of M to integrate over the elements of the matrices $\Lambda = \mathrm{diag}(\lambda_i, \ldots, \lambda_N)$ and U. As in general transformations of coordinates, we include a Jacobian which has to be found:

$$Z = \frac{1}{Vol(U(N))} \int dM f(M) = \int dU \int \prod_i d\lambda_i f(\Lambda) J(\Lambda, U) \quad , \tag{A.1}$$

Where we have used $f(M) = f(\Lambda)$ due to unitary symmetry. In the following we will see that $J(\Lambda, U) = J(\Lambda)$ and then determine its explicit form. Now we construct a new object, namely:

$$\Delta^{-2}(M) = \int_{U(N)} dU \delta^{(2)}[(UMU^{\dagger} - M)_{ij}] \quad , \tag{A.2}$$

Where

$$\delta^{(2)}[(UMU^{\dagger} - M)_{ij})] = \delta[Re(UMU^{\dagger} - M)_{ij}]\delta[Im(UMU^{\dagger} - M)_{ij}] \quad , \tag{A.3}$$

And the integration is taken over the unitary group. The last expression is not unanticipated if one takes into account the way we define the measure dM in (2.2), which is described in terms of diagonal and off-diagonal terms. One might interpret the Δ^2 as the Faddeev-Popov determinant with the eigenvalue playing the gauge fixed condition role. The above defined object can be inserted in the partition function in such a way that (for an explicit form of the unitary group volume see [88])

$$\begin{aligned} Z &= \frac{1}{Vol(U(N))} \int dM f(M) \Delta^2(M) \Delta^{-2}(M) \,, \\ &= \frac{1}{Vol(U(N))} \int dU \int dM f(M) \Delta^2(M)\, \delta^{(2)}[(UMU^{\dagger} - M)_{ij}] \,, \\ &= \frac{1}{N!(2\pi)^N} \int \prod_i d\lambda_i f(\Lambda) \Delta^2(\Lambda) \,, \end{aligned} \tag{A.4}$$

Where the expression outside the integral in the last line is the result of the integration over the unitary group. One can see that indeed $J(\Lambda, U) = J(\Lambda) = \Delta^2(\lambda)$. We now seek an explicit form for $\Delta^2(\Lambda)$. First of all, we express the unitary matrix U by some exponential of an anti-hermitian matrix A. Thereafter:

$$\begin{aligned} U &= e^{-A} \quad \text{and} \quad A^\dagger = -A \quad , \\ U^\dagger \Lambda U &= e^{A}\Lambda e^{-A} = \Lambda + [A,\Lambda] + \frac{1}{2}[A,[A,\Lambda]] + \cdots \quad , \end{aligned} \tag{A.5}$$

Then:

$$\begin{aligned} (U^\dagger \Lambda U - \Lambda)_{ij} &= A_{ik}\Lambda_{kj} - \Lambda_{il}A_{lj} \, , \\ &= (\lambda_j A_{ik}\delta_{kj} - \lambda_i A_{lj}\delta_{il}) = \big(\lambda_j - \lambda_i\big)A_{ij} \, , \end{aligned} \tag{A.6}$$

Where we have used the relation $\Lambda_{ij} = \lambda_i \delta_{ij}$. With this result we can find an explicit expression for the Jacobian:

$$\begin{aligned} \Delta^{-2}(\lambda) &= \int \prod_{i<j}^{N} d(ReA_{ij}) d(ImA_{ij}) \delta\big[Re\big\{(\lambda_j - \lambda_i)A_{ij}\big\}\big] \, \delta\big[Im\big\{(\lambda_j - \lambda_i)A_{ij}\big\}\big] \\ &= \prod_{i<j}^{N} \bigg(\int dA_{ij} \, \delta\big[(\lambda_j - \lambda_i)A_{ij}\big] \bigg)^2 \quad . \end{aligned} \tag{A.7}$$

Using a property of the Dirac's delta function:

$$\delta\big[(\lambda_j - \lambda_i)A_{ij}\big] = \delta A_{ij} \bigg| \frac{d}{dA_{ij}} \big[A_{ij}(\lambda_j - \lambda_i)\big] \bigg|^{-1} , \tag{A.8}$$

We understand that,

$$\prod_{i<j}^{N} \bigg(\int dA_{ij} \, \frac{\delta A_{ij}}{\big|\lambda_j - \lambda_i\big|} \bigg)^2 = \prod_{i<j}^{N} \bigg(\int dA_{ij} \delta A_{ij} \bigg)^2 \big|\lambda_j - \lambda_i\big|^{-2} \quad , \tag{A.9}$$

Yielding,

$$\Delta(\lambda) = \prod_{i<j}^{N} \big(\lambda_j - \lambda_i\big). \tag{A.10}$$

The above expression is known to be the Vandermonde's determinant, given by:

$$\Delta(\lambda) = det(\lambda_i^j) \, . \tag{A.11}$$

Now we are able prove the equivalence between (A.10) and (A.11) . The procedure consists of applying the property of matrices which assures they do not change under linear combinations of either columns or arrows. The determinant is written as

$$det(\lambda_i^j) = \begin{vmatrix} 1 & \lambda_1 & \cdots & \lambda_1^{n-2} & \lambda_1^{n-1} \\ 1 & \lambda_2 & \cdots & \lambda_2^{n-2} & \lambda_2^{n-1} \\ 1 & \lambda_{n-1} & \cdots & \lambda_{n-1}^{n-2} & \lambda_{n-1}^{n-1} \\ 1 & \lambda_n & \cdots & \lambda_n^{n-2} & \lambda_n^{n-1} \end{vmatrix} .$$

We can then apply the property needed: one multiplies the first column by $(-\lambda_1)$ and then sum it to the second. If we do the same to all other columns, we obtain

$$det(\lambda_i^j) = \prod_{p=2}^{n}(\lambda_p - \lambda_1) \begin{vmatrix} 1 & \lambda_2 & \cdots & \lambda_2^{n-3} & \lambda_2^{n-2} \\ 1 & \lambda_3 & \cdots & \lambda_3^{n-3} & \lambda_3^{n-2} \\ \vdots & \vdots & \ddots & \vdots & \vdots \\ 1 & \lambda_{n-1} & \cdots & \lambda_{n-1}^{n-3} & \lambda_{n-1}^{n-2} \\ 1 & \lambda_n & \cdots & \lambda_n^{n-3} & \lambda_n^{n-2} \end{vmatrix} .$$

Thus, we can use mathematical induction to go further, that is:

$$\begin{aligned} det(\lambda_i^j) &= \prod_{p_2=2}^{n} \cdots \prod_{p_n=n}^{n} (\lambda_{p_2} - \lambda_1) \cdots (\lambda_{p_n} - \lambda_{n-1}) \quad , \\ &= \prod_{1 \le i < j \le n} (\lambda_j - \lambda_i) = \prod_{i<j} (\lambda_j - \lambda_i) \quad . \end{aligned} \tag{A.12}$$

B
Matrix integrals

In this appendix we shall prove that (2.17) and (2.19) holds. We start with the average of a new object, precisely:

$$\langle e^{p_k x_k}\rangle = \frac{1}{Z_0}\int_{-\infty}^{+\infty} dx_k\, e^{-\frac{x_k^2}{2}}\, e^{p_k x_k} \quad , \quad Z_0 = \sqrt{2\pi} \quad . \tag{B.1}$$

We want to find a connection between (B.1) and (2.17). First we take the derivative of (B.1) relative to p_i:

$$\begin{aligned}\frac{\partial}{\partial p_i}\langle e^{p_k x_k}\rangle &= \frac{1}{Z_0}\int_{-\infty}^{+\infty} dx_k\, e^{-\frac{x_k^2}{2}}\left(x_k\frac{\partial p_k}{\partial p_i}\, e^{p_k x_k}\right) \quad , \\ &= \frac{1}{Z_0}\int_{-\infty}^{+\infty} dx_k\, e^{-\frac{x_k^2}{2}}\, x_k\delta_{ki}\, e^{p_k x_k} \quad . \end{aligned} \tag{B.2}$$

We take the derivative once again, only that this time it will be relative to p_j :

$$\begin{aligned}\frac{\partial}{\partial p_j}\frac{\partial}{\partial p_i}\langle e^{p_k x_k}\rangle &= \frac{1}{Z_0}\int_{-\infty}^{+\infty} dx_k\, e^{-\frac{x_k^2}{2}}\, x_i\left(x_k\frac{\partial p_k}{\partial p_j}\, e^{p_k x_k}\right) \quad , \\ &= \frac{1}{Z_0}\int_{-\infty}^{+\infty} dx_k\, e^{-\frac{x_k^2}{2}}\, x_i x_k\delta_{kj}\, e^{p_k x_k} \quad , \\ &= \frac{1}{Z_0}\int_{-\infty}^{+\infty} dx_k\, e^{-\frac{x_k^2}{2}}\, x_i x_j\, e^{p_k x_k} \quad . \end{aligned} \tag{B.3}$$

Well, it is straightforward to see that if we set $p_k = 0$ we recover the two-point average is recovered, that is (see (2.16)):

$$\frac{\partial}{\partial p_j}\frac{\partial}{\partial p_i}\langle e^{p_k x_k}\rangle\Big|_{p_k=0} = \frac{\partial}{\partial p_j}\frac{\partial}{\partial p_i} e^{p_k^2/2}\Big|_{p_k=0} = \langle x_i x_j\rangle \quad . \tag{B.4}$$

Therefore:

$$\frac{\partial}{\partial p_j}\left(p_k\frac{\partial p_k}{\partial p_i}\right)e^{p_k^2/2}\Big|_{p_k=0} = \frac{\partial}{\partial p_j}\left(p_k\delta_{ki}\right)e^{p_k^2/2}\Big|_{p_k=0} = \frac{\partial p_k}{\partial p_j}\delta_{ki} \quad , \tag{B.5}$$

Ergo,

$$\langle x_i x_j\rangle = \delta_{ki}\delta_{jk} = \delta_{ij} \quad , \tag{B.6}$$

Which assures that (2.17) holds. Now we apply this method to matrices. It is easy to check the following,

$$\langle e^{\mathrm{tr}SM}\rangle = \frac{1}{Z_0}\int_{-\infty}^{+\infty} dM\, e^{-\frac{N}{2}\mathrm{tr}M^2}\, e^{\mathrm{tr}SM} = e^{S^2/2N} \tag{B.7}$$

Once more, we perform the derivatives:

$$\frac{\partial}{\partial S_{ij}}\langle e^{\mathrm{tr}SM}\rangle = \frac{1}{Z_0}\int_{-\infty}^{+\infty} dM\, e^{-\frac{N}{2}\mathrm{tr}M^2}\left(\frac{\partial}{\partial S_{ij}} e^{\mathrm{tr}SM}\right) \quad , \tag{B.8}$$

Notice that,

$$\mathrm{tr}(SM) = \sum_a S_{ab}M_{ba} \quad , \tag{B.9}$$

Yielding:

$$\begin{aligned}\frac{\partial}{\partial S_{ij}}\langle e^{\mathrm{tr}SM}\rangle &= \frac{1}{Z_0}\int_{-\infty}^{+\infty} dM\, e^{-\frac{N}{2}\mathrm{tr}M^2}\left(M_{ba}\frac{\partial S_{ab}}{\partial S_{ij}}\, e^{\mathrm{tr}SM}\right) \quad , \\ &= \frac{1}{Z_0}\int_{-\infty}^{+\infty} dM\, e^{-\frac{N}{2}\mathrm{tr}M^2}\left(M_{ba}\delta_{aj}\delta_{bi}\, e^{\mathrm{tr}SM}\right) \quad . \end{aligned} \tag{B.10}$$

Taking another derivative (respective to S_{kl}) we acquire:

$$\begin{aligned}\frac{\partial}{\partial S_{kl}}\frac{\partial}{\partial S_{ij}}\langle e^{\mathrm{tr}SM}\rangle &= \frac{1}{Z_0}\int_{-\infty}^{+\infty} dM\, e^{-\frac{N}{2}\mathrm{tr}M^2}\left(M_{ba}\delta_{aj}\delta_{bi}\right)\left(M_{ba}\frac{\partial S_{ab}}{\partial S_{kl}}\, e^{\mathrm{tr}SM}\right) \quad , \\ &= \frac{1}{Z_0}\int_{-\infty}^{+\infty} dM\, e^{-\frac{N}{2}\mathrm{tr}M^2}\left(M_{ba}\delta_{aj}\delta_{bi}\right)\left(M_{ba}\delta_{al}\delta_{bk}\right) e^{\mathrm{tr}SM} \quad , \\ &= \frac{1}{Z_0}\int_{-\infty}^{+\infty} dM\, e^{-\frac{N}{2}\mathrm{tr}M^2}\, M_{ij}M_{kl}\, e^{\mathrm{tr}SM} \quad , \end{aligned} \tag{B.11}$$

Thereupon,

$$\frac{\partial}{\partial S_{kl}}\frac{\partial}{\partial S_{ij}}\langle e^{\mathrm{tr}SM}\rangle\Big|_{S=0} = \frac{\partial}{\partial S_{kl}}\frac{\partial}{\partial S_{ij}} e^{S^2/2N}\Big|_{S=0} = \langle M_{ij}M_{kl}\rangle \quad . \tag{B.12}$$

It follows (we write $S^2 = S_{ij}S_{jq}$),

$$\begin{aligned}\langle M_{ij}M_{kl}\rangle &= \frac{\partial}{\partial S_{kl}}\left[\frac{1}{2N}\left(S_{jq} + S_{ij}\frac{\partial S_{jq}}{\partial S_{ij}}\right)e^{S^2/2N}\right]_{S=0} \quad , \\ &= \frac{1}{2N}\frac{\partial}{\partial S_{kl}}\left[\left(S_{jq} + S_{ij}\delta_{qi}\right)e^{S^2/2N}\right]_{S=0} \quad , \\ &= \frac{1}{2N}\left(\frac{\partial S_{jq}}{\partial S_{kl}} + \frac{\partial S_{ij}}{\partial S_{kl}}\delta_{qi}\right) = \frac{1}{2N}\left(\delta_{jl}\delta_{qk} + \delta_{ik}\delta_{jl}\delta_{qi}\right) \quad , \\ &= \frac{1}{2N}\left(\delta_{jl}\delta_{ik} + \delta_{ik}\delta_{jl}\right) = \frac{1}{N}\delta_{ik}\delta_{jl} \quad , \end{aligned} \tag{B.13}$$

Showing that (2.19) holds as well.

C
Orthogonal polynomials formulas

In this appendix we prove that equations (4.40) and (4.45) holds. Afterwards, we shall compute the free energy for different potentials and find the explicit form of $a_e^2, a_l^2, s_e(1), s_l(1)$ as well.

C.1
Partition function from recursion relations

It is possible to express the elements of the matrix in terms of each polynomial $P_n(\lambda)$. Using the property of matrices in which adding columns to another column does not change the determinant, we rewrite the Vandermonde's determinant (Appendix A):

$$\Delta(\lambda) = \begin{vmatrix} P_0(\lambda_1) & P_1(\lambda_1) & \cdots & P_{n-1}(\lambda_1) \\ P_0(\lambda_2) & P_1(\lambda_2) & \cdots & P_{n-1}(\lambda_2) \\ \vdots & \vdots & \ddots & \vdots \\ P_0(\lambda_n) & P_1(\lambda_n) & \cdots & P_{n-1}(\lambda_n) \end{vmatrix} = det\Big(P_{j-1}(\lambda_i)\Big).$$

Now we should revise the partition function with the help of orthogonal polynomials. To do that one has first to compute the Vandermonde's determinant in the polynomial fashion. We start with determinant definitions:

$$det\Big(P_{j-1}(\lambda_i) = \epsilon^{i_1\cdots i_n} V_{1i_1}\cdots V_{ni_n} = \epsilon^{i_1\cdots i_n} P_{i_1-1}(\lambda_1)\cdots P_{i_n-1}(\lambda_n) \quad . \tag{C.1}$$

Plugging it into (A.4) (Recall A.12), we acquire:

$$Z = \frac{1}{N!(2\pi)^N}\int \prod_{i=1}^{N} d\lambda_i f(\lambda)\left[\epsilon^{i_1 i_2\cdots i_N}\prod_{k=1}^{N} P_{i_k-1}(\lambda_k)\right]^2 \quad , \tag{C.2}$$

Which can be rewritten as

$$\begin{aligned} &= \frac{1}{N!}\int \prod_{i=1}^{N}\frac{d\lambda_i}{2\pi} f(\lambda)\left[\epsilon^{i_1 i_2\cdots i_N}\prod_{k=1}^{N} P_{i_k-1}(\lambda_k)\epsilon^{j_1 j_2\cdots j_N}\prod_{k=1}^{N} P_{j_k-1}(\lambda_k)\right], \\ &= \frac{1}{N!}\epsilon^{i_1 i_2\cdots i_N}\epsilon^{j_1 j_2\cdots j_N}\left[\int \prod_{k=1}^{N}\frac{d\lambda_k}{2\pi} f(\lambda) P_{i_k-1}(\lambda_k) P_{j_k-1}(\lambda_k)\right], \end{aligned} \tag{C.3}$$

After careful algebra we find (because $\epsilon^{i_1 i_2 \cdots i_k}\epsilon_{i_1 i_2 \cdots i_k} = k!$):

$$Z = \frac{1}{N!}\left[\epsilon^{i_1 i_2 \cdots i_N}\epsilon^{i_1 i_2 \cdots i_N}\prod_{k=1}^{N} h_{i_k - 1}\right] = \prod_{k=1}^{N} h_{i_k - 1} \quad . \tag{C.4}$$

Applying (4.36) to the above result we obtain:

$$Z = \prod_{i=1}^{N-1} h_i = h_0^N \prod_{i=1}^{N} r_i^{N-i} \quad . \tag{C.5}$$

C.2
String equations

We have found a better way to compute the partition function using the orthogonal polynomials. So, is necessary to figure out some sort of equation in which r_i can be found. From basic properties of the polynomials one can see that:

$$\lambda P_n'(\lambda) \sim n\lambda^n \quad \therefore \quad \int d\mu\, \lambda\, P_n'(\lambda) P_n(\lambda) = n h_n \quad . \tag{C.6}$$

From (4.36) we obtain,

$$r_n \int d\mu\, P_n'(\lambda) P_{n-1}(\lambda) = n h_n \quad . \tag{C.7}$$

One quickly realizes that the following relations holds:

$$\int d\lambda f(\lambda) P_{n-1} P_n = 0 \quad , \quad \frac{d}{d\lambda}\left[\int d\lambda f(\lambda) P_{n-1} P_n\right] = 0 \quad . \tag{C.8}$$

Thus,

$$\int d\lambda f'(\lambda) P_{n-1} P_n = -\int d\mu P_{n-1} P_n' \quad . \tag{C.9}$$

Another relations we want to mention are:

$$\begin{aligned} \frac{d}{d\lambda}\left[\int d\lambda f(\lambda) P_n(\lambda) P_n(\lambda)\right] = \frac{dh_n}{d\lambda} &= 0 \quad , \\ \int d\lambda f'(\lambda)\, P_n(\lambda)\, P_n(\lambda) &= 0 \end{aligned} \tag{C.10}$$

We rewrite (C.7) and (C.10) as:

$$\begin{aligned} n h_n &= r_n \int d\lambda\, P_{n-1}(\lambda)\, f'(\lambda)\, P_n(\lambda) \quad , \\ 0 &= \int d\lambda\, P_n(\lambda)\, f'(\lambda)\, P_n(\lambda) \quad . \end{aligned} \tag{C.11}$$

These are the string equations. In order to match (4.45) one simply has to choose $f(\lambda) = e^{-(N/t)V(\lambda)}$.

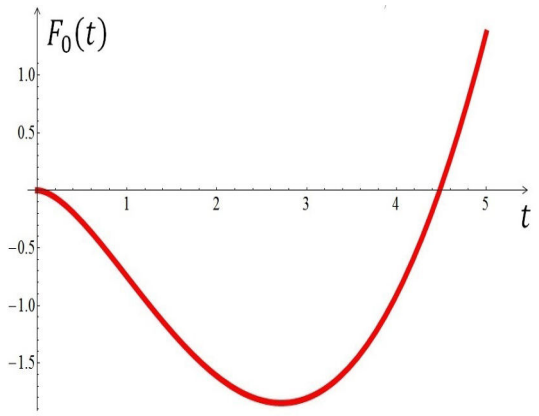

Figure C.1: Free Energy of a Gaussian potential.

C.3
Free energy

In this section we aim to find the free energy for a particular choice of the potential $V(\lambda)$. Hereinafter, we shall use the string equations and the recursion relations, in such a way that we find an expression for r_n. We start with the simplest one, the Gaussian potential:

$$\begin{aligned}\frac{nh_n t}{N} &= r_n \int d\mu\big(\lambda P_{n-1}(\lambda)\big)\, P_n(\lambda) \quad , \\ &= r_n \int d\mu\big(P_n + r_{n-1}P_{n-2}\big)P_n = r_n h_n \quad , \end{aligned} \tag{C.12}$$

Therefore,

$$\lim_{N\to+\infty} r_n = r(\xi) = \xi t \quad , \tag{C.13}$$

Applying (C.13) unto (4.44) we acquire:

$$F_0(t) = \int_0^t dr\,(t-r)\ln r = \frac{t^2}{4}\big(2\ln t - 3\big) \quad , \tag{C.14}$$

Whose behaviour is depicted in figure C.1. For a quartic potential of the form $V(\lambda) = \frac{1}{2}\lambda^2 - \frac{1}{4}g\lambda^4$ the string equation reads:

$$\begin{aligned}\xi_n \frac{h_n}{r_n} t = \int d\mu\,\big(P_n + r_{n-1}P_{n-2}\big)\,P_n - g\int d\mu\,\Big[\big(P_{n+1} + r_n P_{n-1}\big)\times \\ \big(P_{n+1} + (r_n + r_{n-1})P_{n-1} + r_{n-1}r_{n-2}P_{n-3}\big)\Big] \quad , \\ = h_n - g\big[h_n r_{n+1} + (r_n + r_{n-1})h_n\big] \quad , \end{aligned} \tag{C.15}$$

Being simplified as:

$$\xi_n t = r_n - g r_n\big(r_{n+1} + r_n + r_{n-1}\big)\,. \tag{C.16}$$

Now we apply the large-N limit and obtain:

$$\xi t = r(\xi)\big(1 - 3gr(\xi)\big) \quad . \tag{C.17}$$

Consequently:

$$r^2 - \frac{1}{3g}r + \frac{t}{3g}\xi = 0 \quad \therefore \quad r(\xi) = \frac{1}{6g}\big(1 \pm \sqrt{1 - 12gt\xi}\big) \quad .$$

We are now obligated to choose the exact intervals of integration in (4.44), since both $r(1)$ and $r(0)$ admit two different values. The way to decide this is by noticing that when g goes to zero those intervals must converge back to the ones of the Gaussian potential. Ergo:

$$\lim_{g\to 0} r(1) = \lim_{g\to 0} \frac{1 + \sqrt{1 - 12gt}}{6g} = +\infty \quad or \quad \lim_{g\to 0} \frac{\frac{d}{dg}\big(1 - \sqrt{1 - 12gt}\big)}{\frac{d}{dg}\big(6g\big)} = t \quad .$$

One could rather take the limit for $r(\xi)$ when g approaches zero and check if (C.13) would be recovered. Indeed we have:

$$\lim_{g\to 0} r(\xi) = \xi t \quad \Leftrightarrow \quad r(\xi) = \frac{1 - \sqrt{1 - 12g\xi t}}{6g} \quad . \tag{C.18}$$

It follows:

$$F_0(t) = \int_0^{\frac{1-\sqrt{1-12gt}}{6g}} dr\,(t - r + 3gr^2)(1 - 6gr)\ln r \quad . \tag{C.19}$$

The free energy of the quartic potential can be written as:

$$F_0(t) = \frac{1}{432g^2}\Bigg\{54g^2t^2\bigg[4\ln\bigg(\frac{1 - \sqrt{1 - 12gt}}{6g}\bigg) - 3\bigg] + \bigg[1 - 36gt + (30gt - 1)\sqrt{1 - 12gt}\bigg]\Bigg\} \quad . \tag{C.20}$$

We are ready to study odd potentials as it is clear that the recursion relations are a little bit different in this case. Let us analyse what happens for a general cubic potential:

$$\xi_n \frac{h_n}{r_n} t = \int d\mu\, P_{n-1}\, \frac{d}{d\lambda}\big(g_1\lambda + \frac{1}{2}\lambda^2 + \frac{1}{3}g_3\lambda^3\big)\, P_n \quad ,$$

Leading to

$$\xi_n t = r_n\Big[1 + g_3(s_n + s_{n-1})\Big] \quad .$$

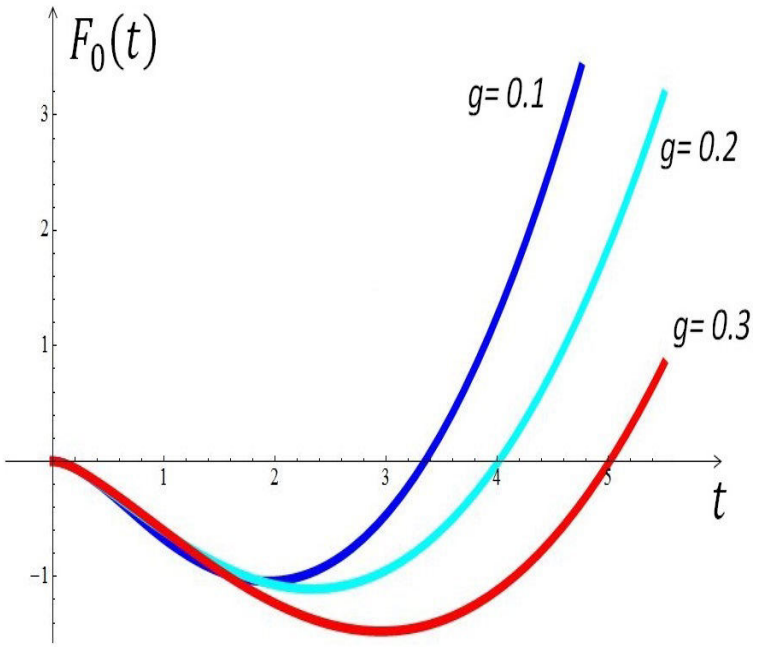

Figure C.2: Free Energy for a quartic potential.

The second recursion relation comes from the second string equation, as follows:

$$0 = g_1 \int d\mu\, P_n P_n + \int d\mu \left(\lambda P_n\right) P_n + g_3 \int d\mu \left(\lambda P_n\right) \left(\lambda P_n\right) \quad ,$$

Thus,

$$0 = g_1 + s_n + g_3\big(r_{n+1} + r_n + s_n^2\big) \quad .$$

In the large-N limit the two string equations become:

$$\xi t = r(\xi)\Big[1 + 2g_3 s(\xi)\Big] \quad ; \quad 0 = g_1 + s(\xi) + g_3\Big[2r(\xi) + s^2(\xi)\Big] \quad . \qquad \text{(C.21)}$$

We now solve the second equation for $s(\xi)$:

$$g_3 s^2 + s + \big(2g_3 r + g_1\big) = 0 \quad \therefore \quad s = -\frac{1}{2g_3}\Big[1 \pm \sqrt{1 - 4g_3\big(2g_3 r + g_1\big)}\Big] \quad ,$$

The solution is,

$$s(\xi) = -\frac{1}{2g_3}\Big[1 - \sqrt{1 - 4g_3(2g_3 r + g_1)}\Big] \quad . \qquad \text{(C.22)}$$

Now we are able to perform (4.44). First, we isolate $r(\xi)$, yielding:

$$\xi = \frac{r}{t}\sqrt{1 - 4g_3(2g_3 r + g_1)} \quad ; \quad 8g_3^2 r^3 + (4g_1 g_3 - 1)r^2 + \xi^2 t^2 = 0 \quad . \qquad \text{(C.23)}$$

There are three solutions, namely:

$$r^{\pm} = \frac{(1-4g_1g_3)}{24g_3^2} - \frac{(1\pm i\sqrt{3})(1-4g_1g_3)^2}{48g_3^2\sqrt[3]{\gamma+\sqrt{\gamma^2-4(1-4g_1g_3)^6}}} -$$

$$\frac{(1\mp i\sqrt{3})\sqrt[3]{\gamma+\sqrt{\gamma^2-4(1-4g_1g_3)^6}}}{48g_3^2} \quad ,$$

$$r^{(0)} = \frac{(1-4g_1g_3)}{24g_3^2} + \frac{(1-4g_1g_3)^2}{24g_3^2\sqrt[3]{\gamma+\sqrt{\gamma^2-4(1-4g_1g_3)^6}}} +$$

$$\frac{\sqrt[3]{\gamma+\sqrt{\gamma^2-4(1-4g_1g_3)^6}}}{24g_3^2} \quad ,$$

$$\gamma = 1 - 12g_1g_3 + 48g_1^2g_3^2 - 64g_1^3g_3^3 - 864g_3^4\xi^2t^2 \quad . \tag{C.24}$$

After carefully taking the limit of all three solutions, turns out that

$$\lim_{g_3,g_1\to 0} r^{\pm}(\xi) = \pm i\sqrt{-\xi^2t^2} \quad ,$$

$$\lim_{g_3,g_1\to 0} r^{(0)}(\xi) = \infty \quad , \tag{C.25}$$

As a result,

$$\lim_{g_3,g_1\to 0} r(\xi) = 0 \quad \Rightarrow \quad r(\xi) = r^{-}(\xi) \quad . \tag{C.26}$$

Notice that r^- is the only solution that plugged into (C.23) also satisfies the condition in which s vanishes for $g_1 = g_3 = 0$. For the DT potential we would have $g_1 = 0$ and $g_3 = -g$, implying:

$$\lim_{g\to 0} \mathfrak{r}^{-}(\xi) = 0 \quad \Rightarrow \quad \mathfrak{r} \equiv \lim_{g_1\to 0} r(\xi)\big|_{g_3=-g} \quad . \tag{C.27}$$

The DT free energy can be found by,

$$F_0(t) = \int_0^{\mathfrak{r}^-} dr\, \frac{(t - r\sqrt{1-8g^2r})(1-4g^2-8g^2r)}{\sqrt{1-8g^2r}} \ln r \quad , \tag{C.28}$$

Moreover, we set $g_1 = g_3 = -g$ to find the free energy in CDT:

$$F_0(t) = \int_0^{r^-} dr\, \frac{(t - r\sqrt{1-4g^2-8g^2r})(1-8g^2-8g^2r)\ln r}{\sqrt{1-4g^2-8g^2r}} \tag{C.29}$$

Furthermore, the values for the functions r and s are:

$$s_e(1) = \frac{1}{2g} - \frac{(1+i\sqrt{3})}{4\sqrt[3]{\alpha_1}} - \frac{(1-i\sqrt{3})\sqrt[3]{\alpha_1}}{12g^2} \quad , \tag{C.30}$$

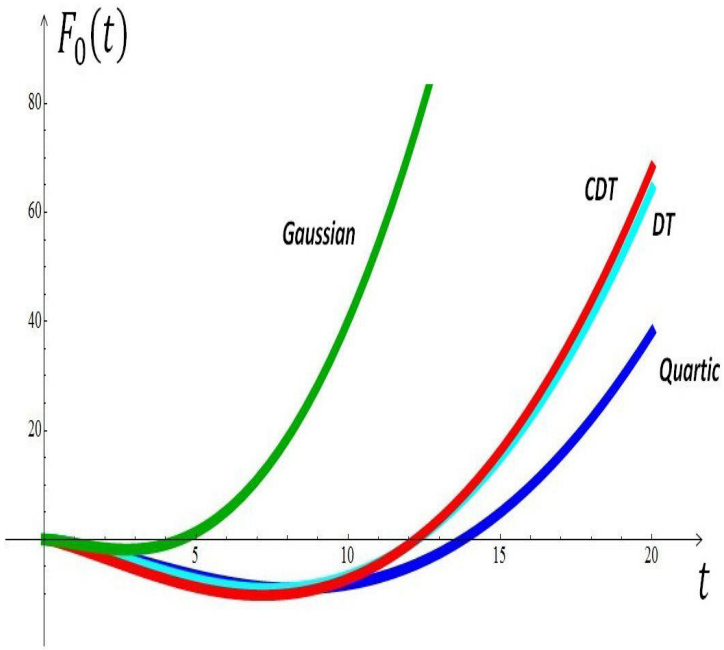

Figure C.3: Free Energies of all four potentials with a fixed parameter $g = 1$.

$$a_e^2 = \frac{1}{6g^2} - \frac{(1-i\sqrt{3})}{12g^2\sqrt[3]{\alpha_2}} - \frac{(1+i\sqrt{3})\sqrt[3]{\alpha_2}}{12g^2} \quad , \tag{C.31}$$

$$\alpha_1 = 108g^5t + 3\sqrt{3}\sqrt[3]{432g^{10}t^2 - g^6} \quad ; \quad \alpha_2 = 1 - 864g^4t^2 + \sqrt{(1-864g^4t^2)^2 - 1} \quad ,$$

$$s_l(1) = \frac{1}{2g} + \frac{(1+i\sqrt{3})(1-4g^2)}{4\sqrt[3]{\gamma_1}} - \frac{(1-i\sqrt{3})\sqrt[3]{\gamma_1}}{12g^2} \quad , \tag{C.32}$$

$$a_l^2 = (1-4g^2)6g^2 - \frac{(1-i\sqrt{3})(1-4g^2)^2}{12g^2\sqrt[3]{\gamma_2}} - \frac{(1+i\sqrt{3})\sqrt[3]{\gamma_2}}{12g^2} \quad , \tag{C.33}$$

$$\gamma_1 = 108g^5t + 3\sqrt{3}\sqrt[3]{432g^{10}t^2 - g^6(1-4g^2)^3} \quad ,$$

$$\gamma_2 = 1 - 12g^2 + 48g^4 - 64g^6 - 864g^4t^2 + \sqrt{(1-864g^4t^2)^2 - 1 + 1728\,t^2(12g^6 - 48g^8 + 64g^{10})} \quad .$$

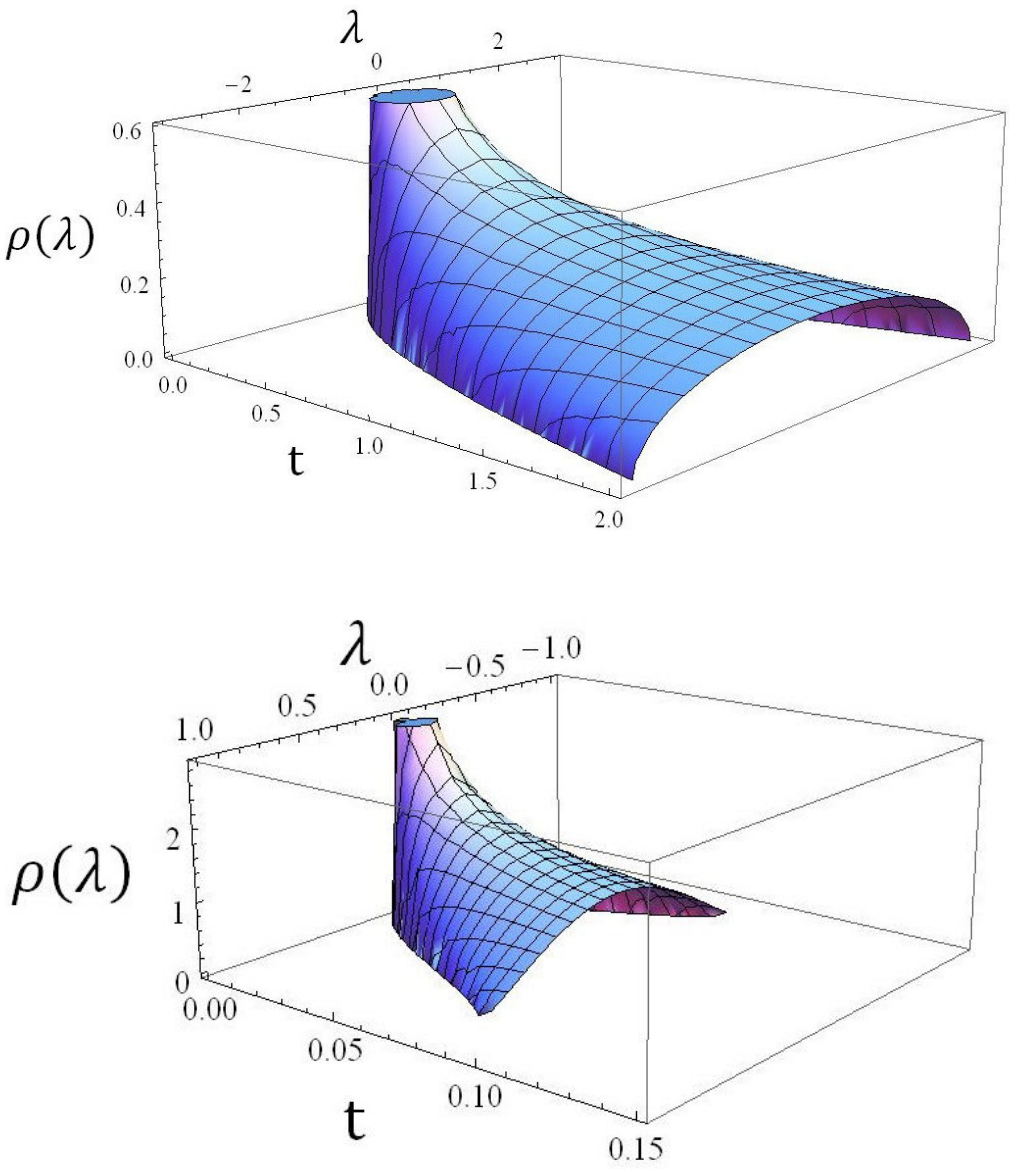

Figure C.4: On the top we see the Gaussian distribution, while the quartic distribution is shown on the bottom.

D
Critical points

In this short appendix we show how to find the critical value of g in DT. Often it is important to find the critical values of the couplings, especially of the g_i encountered within the potential of eigenvalues $V(\lambda)$. Consider the potential equivalent of a dynamical triangulation $V = \frac{1}{2}\lambda^2 - \frac{g}{3}\lambda^3$. For such potential the string equations are

$$g\xi = gr(1-2gs) \quad ; \quad gr = \frac{1}{2}(s - gs^2) \quad . \tag{D.1}$$

We make an expansion around the critical point of $s = s(\xi)$, such that (remember that the critical value of ξ is 1)

$$W(s) \equiv g\xi = g_c + W'(s_c)(s-s_c)^2 + \cdots \quad , \tag{D.2}$$

On the other hand,

$$W(s) = \frac{1}{2}(s - gs^2)(1-2gs) = \frac{1}{2}(s - 3gs^2 + 2g^2s^3) \quad . \tag{D.3}$$

Because we are dealing with only one critical point, it is required that $W'(s_c)$ be equal to zero (D.2). Once this is imposed we arrive at

$$s_c^2 - \frac{1}{g_c}s_c + \frac{1}{6g_c^2} = 0 \quad \therefore \quad s_c = \frac{3 \pm \sqrt{3}}{6g_c} \quad . \tag{D.4}$$

Plugging the previous solution into the second part of (D.1) we obtain

$$r_c = \frac{1}{2g_c}(s_c - gs_c^2) = \frac{1}{12g_c^2} \quad . \tag{D.5}$$

We return once again to (D.1), Note that the role g in the first part is merely a trick (not the g inside the bracket). Removing it and approaching the critical point as well as bearing in mind (D.4), one acquires

$$1 = r_c(1 - 2g_c s_c) \quad \therefore \quad r_c = \mp\sqrt{3} \quad , \tag{D.6}$$

And because g_c is real and having in mind (D.5), yields

$$g_c = \frac{1}{2 \cdot 3^{3/4}} \quad , \quad s_c = \frac{3 - \sqrt{3}}{6g_c} \quad . \tag{D.7}$$

Bibliography

[1] C. Rovelli, *Quantum Gravity*, Cambridge University Press, Cambridge, UK, 2004.

[2] A. Ashtekar and J. Stachel, *Conceptual Problems of Quantum Gravity*, Birkhäuser, Boston, 1991.

[3] C. Kiefer, Conceptual Problems in Quantum Gravity and Quantum Cosmology, *ISRN Math. Phys.*, **2013** (2013) 509316, 1401.3578.

[4] G. E. Gorelik and V. Y. Frenkel, *Matvei Petrovic Bronstein and the Soviet Theoretical Physics in the Thirties*, Birkhäuser Verlag, Boston, 1994.

[5] P. A. M. Dirac, *Lectures on quantum mechanics*, Yeshiva University Press, 1964.

[6] R. Arnowitt, S. Deser and C.W. Misner, The Dynamics of General Relativity, *Gen. Rel. Grav.*, **40** (2008) 1997-2027, gr-qc/0405109v1.

[7] A. Peres, On Cauchy's problem in general relativity - II, *Nuovo Cim.*, **26** (1962) 53-62 .

[8] B. DeWitt , Quantum Theory of Gravity. 1. The Canonical Theory, *Phys. Rev.*, **160** (1967) 1113-1148 .

[9] A. Ashtekar, New Variables for Classical and Quantum Gravity, *Phys. Rev. Lett.*, **57** (1986) 2244-2247 .

[10] T. Jacobson and L. Smolin, Nonperturbative Quantum Geometries, *Nucl. Phys.*, **B331** (1990) 80-152 .

[11] C. Rovelli and L. Smolin, Loop Space Representation of Quantum General Relativity , *Nucl. Phys.*, **B331** (1990) 80-152 .

[12] M. Bojowald, Loop Quantum Cosmology I: Kinematics, *Class. Quant. Grav.*, **17** (2000) 1489-1508, gr-qc/9910103.

[13] J. Brunnemann and T. Thiemann, On (Cosmological) Singularity Avoidance in Loop Quantum Gravity, *Class. Quant. Grav.*, **23** (2006) 1395-1428, gr-qc/0505032.

[14] A. Ashtekar, Loop Quantum Cosmology: An Overview, *Gen. Rel. Grav.*, **41** (2009) 707-741, 0812.0177.

[15] G. 't Hooft and M.J.G. Veltman, One loop divergencies in the theory of gravitation, *Annales Poincare Phys. Theor.*, **A20** (1974) 69-94 .

[16] J. H. Schwarz, The Early History of String Theory and Supersymmetry, 1201.0981.

[17] J. Polchinski, Dirichlet-Branes and Ramond-Ramond Charges, *Phys. Rev. Lett.*, **75** (1995) 4724-4727, hep-th/9510017.

[18] A. Strominger and C. Vafa, Microscopic Origin of the Bekenstein-Hawking Entropy, *Phys. Lett. B*, **379** (1996) 99-104 , hep-th/9601029.

[19] J. Maldacena, The Large N Limit of Superconformal Field Theories and Supergravity, hep-th/9711200.

[20] R. Penrose, Twistor theory: An Approach to the quantization of fields and space-time, *Phys. Rept.*, **6** (1972) 241-315 .

[21] E. Witten, Perturbative gauge theory as a string theory in twistor space, *Commun. Math. Phys.*, **252** (2004) 189-258, hep-th/0312171.

[22] L.J. Mason, Twistor actions for non-self-dual fields: A Derivation of twistor-string theory, *JHEP*, **0510** (2005) 009, hep-th/0507269.

[23] L.J. Mason and D. Skinner, Heterotic twistor-string theory, *Nucl. Phys.*, **B795** (2008) 105-137, 0708.2276.

[24] M. Bullimore, L.J. Mason and D. Skinner, Twistor-Strings, Grassmannians and Leading Singularities, *JHEP*, **1003** (2010) 070, 0912.0539.

[25] R. Sorkin, Causal sets: Discrete gravity, gr-qc/0309009.

[26] O. Lauscher and M. Reuter, Ultraviolet fixed point and generalized flow equation of quantum gravity, *Phys. Rev.*, **D65** (2002) 025013, hep-th/0108040.

[27] D. Oriti, The Group field theory approach to quantum gravity, gr-qc/0607032.

[28] A. Connes, M.R. Douglas and A. Schwarz, Noncommutative geometry and matrix theory: Compactification on tori, *JHEP*, **9802** (1198) 003, hep-th/9711162.

[29] M. Roček and R. Williams, Quantum Regge Calculus, *Phys. Lett.*, **B104** (1981) 31-37 .

[30] P. Hořava, Quantum Gravity at a Lifshitz Point, *Phys. Rev.*, **D79** (2009) 084008, 0901.3775.

[31] T.P. Sotiriou, Horava-Lifshitz gravity: a status report, *J. Phys. Conf. Ser.*, **283** (2011) 012034, 1010.3218.

[32] E. Kiritsis and G. Kofinas, Horava-Lifshitz Cosmology, *Nucl. Phys.*, **B821** (2009) 467-480, 0904.1334.

[33] P. Hořava, Spectral Dimension of the Universe in Quantum Gravity at a Lifshitz Point, *Phys. Rev. Lett.*, **102** (2009) 161301, 0902.3657.

[34] A. Perez, Spin foam models for quantum gravity, *Class. Quant. Grav.*, **20** (2003) R43, gr-qc/0301113.

[35] G. Gibbons and S. Hawking, *Euclidean Quantum Gravity*, World Scientific, 1993.

[36] J. Ambjorn, B. Durhuus and J. Frohlich, Diseases of Triangulated Random Surface Models, and Possible Cures, *Nucl. Phys. B*, **257** (1985) 433-449 .

[37] J. Ambjorn, Quantization of Geometry, hep-th/9411179.

[38] J. Ambjorn, J. Jurkiewicz and R. Loll, Lorentzian and Euclidean Quantum Gravity - Analytical and Numerical Results, hep-th/0001124.

[39] S. Zohren, A Causal Perspective on Random Geometry, 0905.0213.

[40] S. Zohren, Analytic Results in 2D Causal Dynamical Triangulations: A Review, hep-th/0609177v1.

[41] J. Ambjorn, J. Jurkiewicz and R. Loll, Causal Dynamical Triangulations and the Quest for Quantum Gravity, 1004.0352.

[42] J. Ambjorn, J. Jurkiewicz and R. Loll, Quantum Gravity as sum over Spacetimes, *Lect. Notes Phys.*, **807** (2010) 59-124, 0906.3947.

[43] J. Ambjorn, B. Durhuus and T. Jonsson, Three-Dimensional Simplicial Quantum Gravity And Generalized Matrix Models, *Mod. Phys. Lett. A*, **6** (1991) 1133-1146 .

[44] J. Ambjorn and J. Jurkiewicz, Four-dimensional simplicial quantum gravity, *Phys. Lett. B*, **278** (1992) 42-50.

[45] J. Ambjorn, J. Jurkiewicz and R. Loll, Non-perturbative 3D Lorentzian Quantum Gravity, *Phys. Rev. D*, **64** (2001) 044011, hep-th/0011276.

[46] J. Ambjorn, J. Jurkiewicz and R. Loll, Emergence of a 4D World from Causal Quantum Gravity, *Phys. Rev. Lett.*, **93** (2004), hep-th/0404156.

[47] J. Ambjorn, A. Gorlich, S. Jordan, J. Jurkiewicz and R. Loll, CDT meets Horava-Lifshitz gravity, *Phys. Lett.*, **B690** (2010) 413-419, 1002.3298.

[48] C. Anderson, S.J. Carlip, J.H. Cooperman, P. Hořava, R.K. Kommu and P.R. Zulkowski, Quantizing Hořava-Lifshitz Gravity via Causal Dynamical Triangulations, *Phys. Rev.*, **D85** (2012) 044027, 1111.6634.

[49] J. Ambjorn, L. Glaser, Y. Sato and Y. Watakibi, 2d CDT is 2d Horava-Lifshitz quantum gravity, *Phys. Lett.*, **B722** (2013) 172-175, 1302.6359.

[50] P. Di Francesco, P. Ginsparg and J. Zinn-Justin, 2D Gravity and Random Matrices, *Phys. Rept.*, **254** (1995) 1-133, hep-th/9306153v2.

[51] P. Ginsparg and G. Moore, Lectures on 2D Gravity and 2D String Theory, hep-th/9304011v1.

[52] E. J. Martinec, The Annular Report on Non-critical String Theory, hep-th/0305148v2.

[53] J. Ambjorn and R. Loll, Non-Perturbative Lorentzian Quantum Gravity, Causality and Topology Change, *Nucl. Phys.*, **B536** (1998) 407-434, hep-th/9805108.

[54] J. Ginibre, Statistical Ensembles of Complex, Quaternion and Real Matrices, *J. Math. Phys.*, **6** (1965) 440 .

[55] M.L. Mehta, *Random Matrices*, Academic Press, New York, 1967; 3rd Edition, Elsevier, Amsterdam, 2004.

[56] F.J. Dyson, Statistical Theory of the Energy Levels of Complex Systems. I, *J. Math. Phys.*, **3** (1962) 140-156 .

[57] G. Akemann, J. Baik and P. Di Francesco, *The Oxford Handbook of Random Matrix Theory*, Oxford University Press, 2011.

[58] R. Janik, M. Nowak, G. Papp and I. Zahed, Chiral Random Matrix Models in QCD, hep-ph/9812376.

[59] J.J.M. Verbaarschot, QCD, Chiral Random Matrix Theory and Integrability, hep-th/0502029.

[60] G. 't Hooft, A Planar Diagram Theory for Strong Interactions, *Nucl. Phys.*, **B72** (1974) 461.

[61] D. Bessis, C. Itzykson, and J.B. Zuber, Quantum Field Theory Techniques in Graphical Enumeration, *Adv. Appl. Math.*, **1** (1980) 109-157 .

[62] A. Peres, Critique of the Wheeler-DeWitt equation, gr-qc/9704061.

[63] R. Loll, A Discrete History of the Lorentzian Path Integral, *Lect. Notes Phys.*, **631** (2003) 137-171, hep-th/0212340v2.

[64] D. Grumiller and R. Meyer, Ramifications of Lineland, hep-th/0604049.

[65] D. Grumiller, W. Kummer and D.V. Vassilevich, Dilaton Gravity in Two Dimensions, *Phys. Rept.*, **369** (2002) 327-430, hep-th/0204253.

[66] D. Tong, Lectures on String Theory, 0908.0333.

[67] N. Seiberg, Notes On Quantum Liouville Theory And Quantum Gravity, *Prog. Theor. Phys. Suppl.*, **102** (1990) 319-349 .

[68] Y. Nakayama, Liouville Field Theory - A Decade After the Revolution, *Int. J. Mod. Phys. A*, **19** (2004) 2771-2930, hep-th/0402009.

[69] T. Regge, General Relativity Without Coordinates, *Nuovo Cim.*, **19** (1961) 558-571.

[70] M. Weigel, *Vertex Models on Random Graphs*. PhD Thesis, Universität Leipzig, 2002.

[71] J. Ambjorn, B. Durhuus and T. Jonsson, *Quantum Geometry: A Statistical Field Theory Approach*, Cambridge University Press, Cambridge, UK, 1997.

[72] J. Ambjorn, R. Loll, Y. Watabiki, W. Westra and S. Zohren, A Causal Alternative for c=0 Strings, 0810.2503.

[73] M. Kaku, *Strings, conformal fields, and M-theory*, Springer, 2000, New York.

[74] B. Eynard, *Random Matrices*, Saclay-IPht, 2000.

[75] M. Marino, Lectures on Non-perturbative Effects in Large N Gauge Theories, Matrix Models and Strings, *Fortsch. Phys.*, **62** (2014) 455-540, 1206.6272.

[76] M. Hanada, M. Hayakawa, N. Ishibashi, H. Kawai, T. Kuroki, Y. Matsuo and T. Tada, Loops versus matrices: The Nonperturbative aspects of noncritical string, *Prog. Theor. Phys.*, **112** (2004) 131-181, hep-th/0405076.

[77] E. Witten, Topological Gravity, *Phys. Lett.*, **B206** (1998) 601.

[78] J.M.F Labastida, M. Pernici and E. Witten, Topological Gravity in Two-Dimensions, *Nucl. Phys.*, **B310** (1988) 611.

[79] R. Dijkgraaf and E. Witten, Mean Field Theory, Topological Field Theory, and Multimatrix Models, *Nucl. Phys.*, **B342** (1990) 486-522.

[80] R. Dijkgraaf, H.L. Verlinde and E.P. Verlinde, Topological strings in d < 1, *Nucl. Phys.*, **B352** (1991) 59-86.

[81] M. Marino, Les Houches Lectures on Matrix Models and Topological Strings, hep-th/0410165v3.

[82] M. Kontsevich, Intersection theory on the moduli space of curves and the matrix Airy function, *Commun. Math. Phys.*, **147** (1992) 1-23.

[83] D.J. Gross and A.A. Migdal, Nonperturbative Two-Dimensional Quantum Gravity, *Phys. Rev. Lett.*, **64** (1990) 127.

[84] M.R. Douglas and S.H. Shenker, Strings in Less Than One-Dimension, *Nucl. Phys.*, **B335** (1990) 635.

[85] E. Brezin and V.A. Kazakov, Exactly Solvable Field Theories of Closed Strings, *Phys. Lett.*, **B236** (1990) 144-150.

[86] I.K. Kostov, Boundary Correlators in 2D Quantum Gravity: Liouville versus Discrete Approach, *Nucl. Phys.*, **B658** (2003) 397-416, hep-th/0212194.

[87] A. Sato and A. Tsuchiya, ZZ brane amplitudes from matrix models, *JHEP*, **0502** (2005) 032, hep-th/0412201.

[88] A. Morozov, Integrability and matrix models, *Phys. Usp.*, **37** (1994) 1-55, hep-th/9303139v2.